COUNTERMEASURE METHODS FOR HIGH POWER MICROWAVE PULSES

A THESIS SUBMITTED TO
THE GRADUATE SCHOOL OF NATURAL AND APPLIED SCIENCES
OF
MIDDLE EAST TECHNICAL UNIVERSITY

BY

MUHARREM KESKİN

IN PARTIAL FULLFILLMENT OF THE REQUIREMENTS
FOR
THE DEGREE OF MASTER OF SCIENCE
IN
ELECTRICAL AND ELECTRONICS ENGINEERING

JULY 2014

Approval of the thesis:

COUNTERMEASURE METHODS FOR HIGH POWER MICROWAVE PULSES

submitted by **MUHARREM KESKİN** in partial fulfillment of the requirements for the degree of **Master of Science in Electrical and Electronics Engineering Department, Middle East Technical University** by,

Prof. Dr. Canan Özgen
Dean, Graduate School of **Natural and Applied Sciences** _____

Prof. Dr. Gönül Turhan Sayan
Head of Department, **Electrical and Electronics Eng.** _____

Prof. Dr. Şimşek Demir
Supervisor, **Electrical and Electronics Eng. Dept., METU** _____

Examining Committee Members:

Prof. Dr. Canan Toker
Electrical and Electronics Eng. Dept., METU _____

Prof. Dr. Şimşek Demir
Electrical and Electronics Eng. Dept., METU _____

Prof. Dr. Altunkan Hızal
Electrical and Electronics Eng. Dept., METU _____

Prof. Dr. Sencer Koç
Electrical and Electronics Eng. Dept., METU _____

Tuncay Erdöl, Ph.D.
Lead Design Engineer, ASELSAN _____

Date: 22.07.2014

I hereby declare that all information in this document has been obtained and presented in accordance with academic rules and ethical conduct. I also declare that, as required by these rules and conduct, I have fully cited and referenced all material and results that are not original to this work.

Name, Last name : Muharrem KESKİN

Signature :

ABSTRACT

COUNTERMEASURE METHODS FOR HIGH POWER MICROWAVE PULSES

Keskin, Muharrem

M. S., Department of Electrical and Electronics Engineering

Supervisor: Prof. Dr. Şimşek Demir

July 2014, 95 pages

In this thesis, a limiter structure is investigated to decrease the effects of High Power Microwave (HPM) pulses coupled from front-door by using vanadium dioxide (VO_2). To prove that vanadium dioxide can be used as an RF limiter, this structure is examined, realized and measured. Firstly, susceptibility of LNA to HPM pulses is investigated by an experimental setup to determine the destruction threshold levels of LNA technology for direct injection of HPM pulses. Based on these threshold levels, diode limiter technology is examined in terms of power handling capacity and response time. The behaviors of two diode limiters against the HPM attacks are studied to have a general idea about diode technology. As a result of this study, for pulses having high amplitudes and short pulse widths, diode technology is not enough to protect the vulnerable front-end devices like LNA's. Therefore, another limiter structure is needed to handle the HPM pulses. To produce a VO_2 limiter, VO_2 material is synthesized by using two hydrothermal methods. Then, these produced samples are characterized with X-ray diffraction technique and extraction of resistance characteristics. With this obtained material, a limiter is realized and performance of the limiter is measured and discussed.

KEYWORDS: Countermeasure methods for HPM, Vanadium dioxide (VO_2) limiter, Susceptibility of LNA, Hydrothermal synthesis of VO_2

ÖZ

YÜKSEK GÜÇLÜ MİKRODALGA DARBELERİ İÇİN KARŞI TEDBİR YÖNTEMLERİ

Keskin, Muharrem
Yüksek Lisans, Elektrik ve Elektronik Mühendisliği Bölümü
Tez Yöneticisi: Prof. Dr. Şimşek Demir
Temmuz 2014, 95 sayfa

Bu tezde, Yüksek Güçlü Mikrodalga (YGM) darbelerinin ön kapı kublajından kaynaklı etkilerini azaltmak için bir sınırlayıcı yapısı incelenmiştir. Vanadyum dioksit (VO_2)'in bir radyo frekansı sınırlayıcısı olarak kullanılabileceğini ispatlamak için bu yapı incelenmiş, gerçeklenmiş ve ölçülmüştür. YGM darbelerinin doğrudan enjeksiyonunda Düşük Gürültülü Yükselteç (DGY) teknolojisinin bozulma sınır seviyelerini belirlemek için YGM darbelerine karşı DGY'lerin hassasiyetleri bir deney düzeneğiyle incelenmiştir. Bu sınır seviyelerine dayanarak diyot sınırlayıcı teknolojisi, güç kapasitesi ve tepki süresi açısından değerlendirilmiştir. Diyot teknolojisi hakkında genel fikir sahibi olmak için iki diyot sınırlayıcının YGM saldırılarına karşı davranışlarına çalışılmıştır. Bu çalışmaların sonucu olarak yüksek genlikli düşük darbe genişliğindeki darbelerde, diyot teknolojisi DGY'ler gibi hassas ön kat aletlerini korumada yetersiz kalmaktadır. Bu yüzden YGM darbeleriyle baş etmek için başka bir yapıya ihtiyaç duyulmaktadır. VO_2 sınırlayıcı üretmek için iki hidrotermal yöntem kullanılarak VO_2 malzemesi sentezlenmiştir. Daha sonra bu üretilen numuneler, X-ışını kırınımı tekniği ve direnç karakteristiği çıkartımı ile karakterize edilmiştir. Bu elde edilen malzemeyle bir sınırlayıcı gerçeklenmiş ve bu sınırlayıcının performansı ölçülmüş ve tartışılmıştır.

ANAHTAR KELİMELER: YGM için karşı tedbir yöntemleri, Vanadyum dioksit (VO_2) sınırlayıcı, DGY hassasiyeti, VO_2'nin hidrotermal sentezi

To My Wife,

ACKNOWLEDGEMENTS

I would like to express my deepest gratitude to my family for their loving and continued support.

I cannot express enough thanks to my advisor, Prof. Dr. Şimşek Demir for his excellent guiding, caring, patience and encouragement throughout the thesis.

I would like to express my sincere gratitude to Prof. Dr. Gürkan Karakaş for his guidance, support and technical suggestions throughout the study.

I am grateful to ASELSAN A.Ş. for the financial and technical opportunities provided for the completion of this thesis.

I would also like to express my sincere appreciation for Akın Dalkılıç, Keziban Göksu, Ali Özgün, Tuğçe Kırbaş, Tayfun Filci and Mustafa Durukal for their valuable friendship, motivation and help.

I would like to thank TÜBİTAK for providing financial support during the study.

TABLE OF CONTENTS

LIST OF TABLES

TABLES

LIST OF FIGURES

FIGURES

CHAPTER 1

INTRODUCTION

In today's military applications, the susceptibility of electronic devices and systems is very crucial and High Power Microwave (HPM) pulses have been recently used to disturb and damage these systems in military fields. HPM technology threatens vital military systems by interference, damage and destruction of them. Even if some critical military systems malfunction for a short while during an operation, this disruption may cause huge disasters. Therefore, some important precautions against HPM weapons should be taken for national defense.

HPM weapons have not been seen as potential threats and they still seem as preliminary equipments today but it is reported in [1] that there are many researches and developments about HPM weapons in United States, Great Britain and Russia for several years. As a result of their studies, the U.S. Armed Forces already tested and used them in Iraq and Kosovo Wars. Although the military standards for outer disturbances are very high level and advanced, in Iraq War, some of the equipments inside the Iraqi systems were affected and unexpectedly destructed by electrical interference during the HPM attacks.

HPM technology has the ability to generate pulses having very high amplitudes and very short pulse widths. According to [2], the field intensity at the target reaches to 100 kV/m typically whereas the pulse width is about 100 ns. HPM pulses mostly affect the target device through coupling mechanism. This mechanism can be divided into two groups; namely front-door and back-door coupling.

Electromagnetic energy generally enters the system through the holes, power cables and unshielded output devices in back-door coupling. Therefore, it is possible to prevent or decrease the effects of this coupling by increasing the EM shielding. However, in front-door coupling, the electromagnetic energy penetrates to the system through intentional receptors, e.g., antennas. The antennas are designed to collect very low power signals from the environment so they are the most potential targets of HPM pulses. Moreover, the gain of an antenna increases the power of these signals. Thus, even HPM attacks with low output power can damage the systems. Since antenna is an indispensible part of some systems, the components following the antenna should block HPM attack before reaching the sensitive devices. The first component after the antenna is generally a band pass filter that cannot reflect back the front-door coupling if it is in band. Then, a limiter is placed to prevent high amplitude signals, but the response time of generic limiters in industry is not enough to handle this type of threat. Thus, front-door coupling requires special techniques like ultra fast limiting structures.

The objective of this thesis is mainly to propose a method to decrease the effects of HPM pulses coupled from front-door by using vanadium dioxide (VO_2). For this purpose, HPM sources in literature are researched and discussed. Then, vulnerable components in a general receiver system are investigated. After that, the performances of some limiter structures against this threat are evaluated.

Based on the above mentioned content, this thesis is organized in five chapters as follows:

In chapter 2, HPM test facilities of four European countries, HPM weapons of some countries and some HPM weapons used for terrorist applications are introduced in terms of some significant performance parameters. Moreover, the developments of VO_2, atomic structures of VO_2 states and some applications of VO_2 are investigated briefly.

In Chapter 3, in order to determine the destruction threshold levels of LNA technology for direct injection of HPM pulses, a generic LNA is selected from Hittite Microwave Corporation and the performance of this product is evaluated under HPM threats of different pulse widths.

In chapter 4, two limiters based on diode technology, namely TGL2201 and CLA4609 are studied in terms of power handling capacity and response time. These performance parameters are investigated to observe the behavior of diode technology against the HPM attacks.

In chapter 5, the procedures of VO_2 production by using two different hydrothermal methods with oxalic and formic acids are explained in detail. Next, the X-ray diffraction techniques and the extraction of resistance characteristics of these VO_2 samples are mentioned. The results of this characterization process are discussed briefly. Then, the VO_2 limiters designed for coaxial and waveguide structures in the study [3] are examined and the design procedure of the limiter for waveguide structure is described clearly. In addition, the measurements of designed VO_2 limiter are demonstrated and discussed. Finally, this thesis is concluded with evaluation of this study and future work.

CHAPTER 2

LITERATURE RESEARCH

2.1. HPM Test Facilities

HPM systems have been researched and worked on more than 25 years. However, information about most of the systems is not still available. In this part, HPM test facilities of only four European countries explained in [4] are introduced, discussed and compared with each other in terms of different parameters. These test facilities may also give some idea about today's HPM technology. These test facilities of European countries are listed below:

- Swedish Microwave Test Facility (MTF)
- British HPM system (Orion)
- French HPM system (Hyperion)
- German HPM system (Supra)

2.1.1. Swedish Microwave Test Facility (MTF)

The purpose of Swedish Microwave Test Facility is to test aircrafts in a high-intensity radiated field (HIRF) environment [4]. The source of this test facility is a conventional tube. In this system, five different HPM sources are used to generate five frequencies in separate bands. These five frequencies are fixed and they are namely 1.3 GHz in L band, 2.86 GHz in S band, 5.71 GHz in C band, 9.3 GHz in X band and 15 GHz in Ku band. The main advantage of MTF is to be able to produce

frequencies in five radar bands whereas the disadvantage is that these produced frequencies are spot frequencies and cannot be adjustable from time to time. The general features of the Swedish system are given in Table 2-1 in terms of frequency, maximum average power, maximum power, maximum pulse repetition frequency (PRF), maximum pulse duration and peak value of electrical field strength at 15 meters away from the system. In this thesis, the signals at 10 GHz are focused on so the features in X band are more significant than the others and the Swedish MTF has 1 MW maximum power, 3.8 us maximum pulse duration and 10 kV/m of electric field in this band, but there is no information about rise times of produced signals in [4].

Table 2-1 : Characteristic Parameters of MTF [4]

Radar Band	L	S (PCS)	C	X	Ku
f (GHz)	1.30	2.86	5.71	9.30	15.00
Max. Average power (kW)	49	20	5	1	0.28
Max. power (MW)	25	20 (140)	5	1	0.25
Max. PRF (pps)	1000	1000	1000	1000	2100
Max. Pulse duration (μs)	5	5 (0.4)	5	3.8	0.53
Epeak@15 m (kV/m)	30	30 (80)	17	10	6

2.1.2. British HPM System (Orion)

Physical International (PI) designed Orion HPM system [4]. The sources of this system are basically four magretrons. Orion is able to cover 1-3 GHz frequency band with these four magnetrons since the magretrons are tunable and radiate over a 30% bandwidth with a specific tuning technique. The general features of Orion are shown in Table 2-2 in terms of peak power, frequency, pulse duration, PRF,

burst duration and inter burst delay given due to thermal considerations. The remakable specification of this system is definitely 5 GW peak power. Due to this high output power, even a single shot may lead to failure or damage of some basic systems. On the other hand, the pulse duration of produced signal changes from only 100 ns to 500 ns in 50 ns steps.

Table 2-2 : Specifications of the Orion System [4]

Parameter	Specification
Peak power (Pulse Power System)	5 GW
HF-Source	Magnetron
Frequency	1 – 3 GHz
Pulse duration	100 – 500 ns
PRF	Single Shot to 100 Hz
Burst Duration	10 s (Maximum)
Inter Burst Delay	8 minutes (Minimum)

2.1.3. French HPM System (Hyperion)

Unlike MTF and Orion, the French test facility, Hyperion, is not transportable and it radiates in an anechoic chamber [4]. The sources of Hyperion are two magnetrons and two reltrons. Two tunable reltrons can radiate from 0.72 GHz to 1.44 GHz. The Hyperion has 200 ns pulse duration and 40 kV/m electric field strength below 1.44 GHz. Also, one of the magnetrons covers the frequency band from 1.3 GHz to 1.8 GHz whereas the other has the ability of radiation between 2.4 GHz and 3 GHz. The pulse duration and peak value of electric field of the magnetrons in Hyperion are 100 ns and 60 kV/m, respectively. The specifications of Hyperion are also listed in Table 2-3 in terms of frequency, pulse duration, PRF and peak power of electric field strength.

Table 2-3 : Characteristic Parameters of Hyperion [4]

Parameter	Specification
HF-Source	Magnetron
Frequency	1.3 – 1.8 GHz 2.4 – 3.0 GHz
Pulse duration	100 ns
Epeak	60
HF-Source	Reltron
Frequency	0.72 – 1.44 GHz
Pulse duration	200 ns
PRF	1 Hz
Epeak	40 kV/m

2.1.4. German HPM System (Supra)

Supra was upgraded by TITAN Pulse Sciences Division in 2005 [4]. After this upgrade, the sources of Supra are 8 super reltrons as shown in Table 2-4. These additional 4 reltrons enlarge the frequency range of test facility up to 3 GHz. The reltrons in Supra are mechanically tunable in frequency and they have 20% bandwidths around the center frequency, so the first four reltrons are able to cover frequency band from 0.675 GHz to 1.44 GHz. The general properties of Supra are given in Table 2-4 in terms of the similar parameters mentioned in the previous test facilities. From this table, it can be said that the German test facilities have pulse duration longer than 300 ns, 45 kV/m electric field and 100 MW-400 MW peak power.

Table 2-4 : Specifications of Supra [4]

Parameter	Specification
HF-Source	4 Super Reltrons (8*)
Frequency	0.675 –1.44 GHz (3 GHz*)
Pulse Duration	> 300 ns
Epeak @ 15 m	70 kV/m (45 kV/m *)
RF Peak Power	400 MW – 200 MW (100 MW *)
PRF	10 Hz
Max. Shots / Burst	100
3dB Illumination Area	12 m^2 (9 m^2*)

* 2005 Upgrade

2.2. HPM Weapons

After the investigation of four European countries' test facilities, high power microwave weapons developed by the scientists in United States, Soviet Union and Russia are introduced and compared with respect to features of these weapons.

Table 2-5 shows the properties of different HPM weapons. In this table, some important specifications of weapons like power (P), frequency (F), pulse width (τ), converting effectiveness (η) and also nations are shown in separate columns.

Table 2-5 : Some Properties of HPM Weapons [1]

Name of HPM device	P (GW)	F (GHz)	τ (ns)	η (%)	National
Virtual cathode oscillator	1.2	5.9			America
Freedom electronic laser	>1	40		30	America
Axial driven cathode oscillator	7.5	1.17			America
Plasma auxiliary slow wave oscillator	4—8			15-25	America
Single pulse looping-wave oscillator	1.5	8—12.5	60	30	Soviet Union
Looping-wave oscillator	1	10	2	30	Soviet Union
Field radiation oscillator	0.06	7		25	Soviet Union
Looping-wave oscillator	1.5	X band	60	50	Russian
Repeating pulse looping-wave oscillator	1	10	2	30	Russian
Relativity magnetron	0.1		1000		Russian
Improved cyclotron tube	2	12.5	50		Russian
Polarized radiation microwave tube	0.06	7	700	25	Russian

By comparison of the properties in the table, it can be said that the Russian scientists improves some of devices produced in Soviet Union and develops new weapons. For example, single pulse looping-wave oscillator seems the previous version of the looping-wave oscillator since converting effectiveness and pulse repetition property of the device are improved in the second generation weapon. Again, looping-wave oscillator and repeating pulse looping wave oscillator have the same properties except maybe their pulse repetition performances. All of these four HPM weapons operate at X band. Among them, looping-wave oscillator and repeating pulse looping-wave oscillator are the most serious threats for an X-band radar system since they have short pulse width, high PRF and high power of

signals. These oscillators succeed to generate 1 GW and 1.5 GW power with pulse width of 2 ns and 60 ns, respectively. Due to these superior features, even before some of the radar systems do not recognize the existence of these weapons, they may be destroyed by these HPM weapons.

In addition to these high technology systems, some weapons used in terrorist attacks are represented in [5]. Although these terrorist weapons are mobile, they are also very effective for destruction of electronic systems.

Table 2-6 : Weapons used in terrorist attacks [5]

Tube Type	Peak Output Power	Pulse Length	Pulse Repetition Rate	Efficiency	Approximate Weight
Magnetically Isolated Line Oscillator (MILO)	2 GW	140 nS	Single Shot	10%	Tube - 100 kg Total System -- 600-1200 kg
Relativistic Klystron Oscillator (RKO)	1.5 GW	120 nS	Single Shot	30%	Tube - 550 kg Total System -- 600-1000 kg
Reltron	0.6 GW	300 nS	50 Hz	40%	Tube - 60 kg
Relativistic Magnetron	3 GW	80 nS	Single Shot	10%	Tube ≥ 300 kg

Table 2-6 gives some attack weapons used in terrorist operations. In this table, only tube sources are investigated in terms of peak output power, pulse length, pulse repetition length, efficiency and approximate weight while the operational frequencies of the devices are not given. These sources have also short pulse length and high power of signals as other HPM weapons.

In conclusion, this information about HPM systems gives a general idea about researches and developments in HPM technology. Also, when the test facilities of European countries and HPM weapons introduced above are examined, it is observed that HPM systems in literature can produce pulses having peak power in the order of gigawatts and pulse length in the order of nanoseconds at different frequencies. The countermeasure methods for HPM systems should minimize the effects of these pulses.

2.3. Developments and Applications of Vanadium Dioxide

After HPM technology is investigated briefly, some background information about VO_2 material is also represented in this chapter. Firstly, the discovery of electrical phase transition of VO_2 and atomic structures of different phases are explained and then some applications of VO_2 are introduced in this part.

First of all, a reversible phase transition of vanadium dioxide was discovered by F. J. Morin in 1959 [6]. At a critical temperature, about 68°C, the resistivity of the material changes in the order of 10^3-10^5 as shown in Figure 2-1. Also, the electrical resistance of the material shows hysteresis behavior since the temperature of semiconductor-metal transition is slightly different than the one of reverse transition.

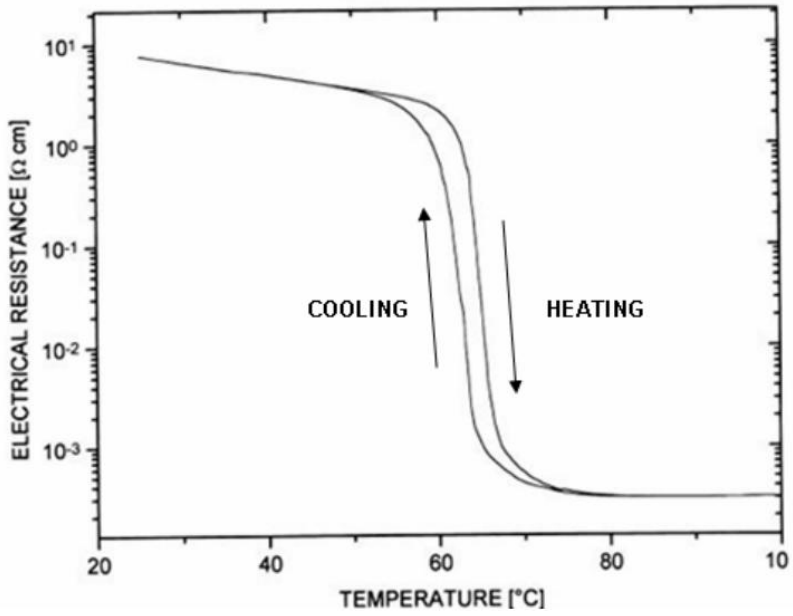

Figure 2-1 : Resistivity of VO_2 as a function of temperature [6]

Below the critical temperature, VO_2 behaves as an insulating material and the resistivity is very high whereas the properties of VO_2 reverse totally and the material seems like a conductor above the critical temperature. In order to understand this interesting behavior, the atomic structures of these two states are

investigated and compared to each other in [7],[8]. The main reason of this behavior is that vanadium dioxide is in monoclinic phase (zig-zag chain) below the critical temperature and in tetragonal or rutile phase (straight chain) above the transition temperature. The lattices of these two phases are illustrated in Figure 2-2. In this demonstration, subscript of B shows atom in the paper plane and subscript A means that atom is behind the paper plane while subscript C corresponds that atom is front of the paper plane. After this transition from monoclinic phase to tetragonal phase, the volume of the material changes slightly and approximately one exceeding electron per V atom occupies a special band that provides the metallic conductivity [8]. Therefore, these exceeding electrons highly increase the conductivity of the material. The physical and electronic structures of VO_2 are not the concern of this thesis and these topics are explained in detail in [7],[8],[9].

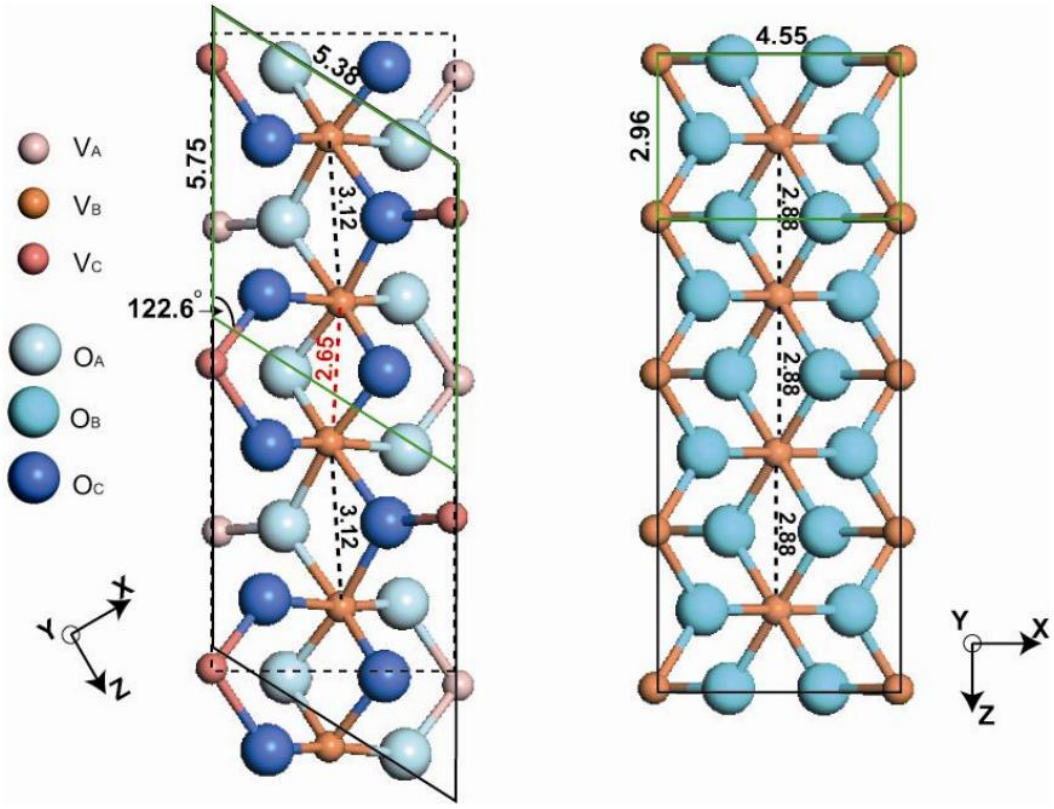

Figure 2-2 : Lattices of two phases of VO_2 (Left: Monoclinic Phase. Right: Rutile Phase) [7]

After Morin's study, all V_xO_y materials have been investigated for several years. Most of these vanadium oxides are classified in terms of color, transition temperature (T_t) and melting temperature(T_m) in [8] and it is understood that all vanadium oxides have the property of transition from semiconductor to conductor but according to oxygen contents of the material, the transition temperatures change as shown in Table 2-7.

Table 2-7 : Some properties of VxOy materials [8]

Compound	T_t	Color	T_m
VO	-147°C [5]	grey [32]	
V_2O_3	-105°C [33]	black [32]	1970°C [32]
V_5O_9	-138°C [7]		
VO_2	+67°C [34]	dark blue [35]	1967°C [32]
V_6O_{13}	-123°C [36]		700°C [37]
V_2O_5	+375°C [38]	yellow [56]	685°C [37]

Due to this significant transition property, VO_2 has been used in many applications such as optical switches, IR and RF shutters, window coatings, filters, limiters, sensors, etc. Some of these applications are explained in this part.

The first application is a VO_2 microwave switch that is introduced in [10]. In this paper, a VO_2 switch compatible with GaAs IC technology is designed. The working principal of this switch depends on high resistivity change of VO_2 material at the transition temperature.

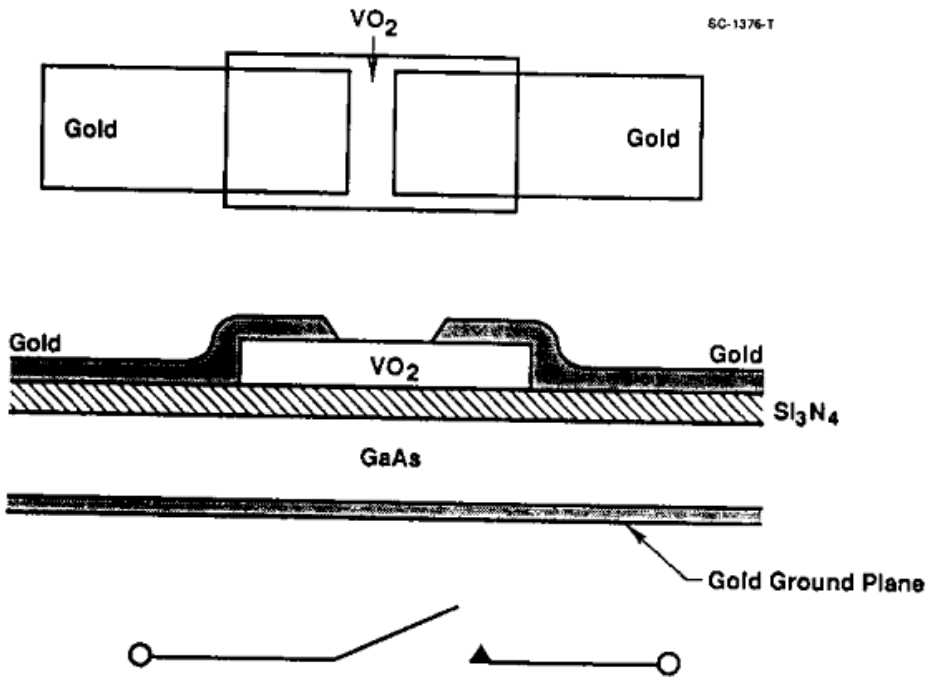

Figure 2-3 : Structure of VO_2 switch [10]

The structure of VO_2 switch is basically illustrated in Figure 2-3. In this figure, a transmission line is designed on a GaAs substrate and this line is interrupted by a gap covered by a VO_2 patch. The switch is activated by using a tungsten heater. When VO_2 is turned from insulating phase to conducting phase by the help of this heater, the switch begins to allow signal transmission. The performance of this switch based on VO_2 thickness and gap dimensions. It is asserted that the response time of the switch is about 30 ns and the switch does not have breakdown and bias restrictions. Also if it is designed appropriately, it can switch very large signals.

Secondly, Daniel Johansson proposed a method to design an active infrared shutter by using VO_2 films [8]. In this study, VO_2 films on sapphire (Al_2O_3) substrate are produced by spin coating method and a heater is assembled to this structure to reduce the switching time of shutter as demonstrated in Figure 2-4. In this illustration, the direction of light is perpendicular to the plane of paper. As a result of this study, it is claimed that switching time of this optical shutter reaches to 15

ms at best and the final component provides a closed transmittance of below 0.1% whereas it transmits 55% of the incident light in the open mode.

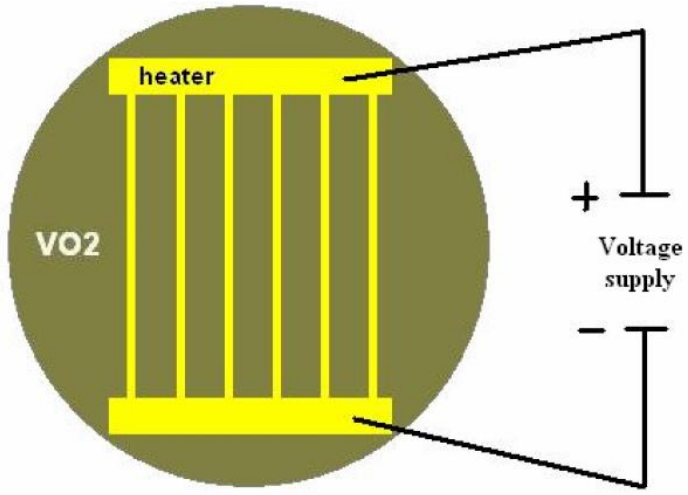

Figure 2-4 : Top view of optical IR shutter [8]

Then, two tunable filter designs in X band are introduced with the combination of split ring resonators (SRR) and VO_2 switches in [11]. One of the main advantages of these devices is that switching time of the filter is improved by using VO_2 switches. In this paper, a four-pole band-stop filter and then a digitally tuned band-reject filter are explained, respectively.

2.4. Countermeasure Methods of HPM

In order to overcome the HPM sources, some methods have been presented in literature. A few applications to protect the electronic systems against HPM are explained in this part.

Energy selective surface (ESS), developed with super-dense diode arrays, is proposed as a method for HPM protection in [12] although response time and insertion loss of the device are need to be optimized.

A tunable passive limiter is introduced to get protection for HPM threats in [13]. This limiter is based on a metamaterial structure, the split-ring resonator (SRR) in this study. However, the response time of the device is not sufficient again.

A vanadium dioxide front end advanced shutter device is represented in [3]. In this patent, two vanadium dioxide limiters suitable for coaxial cables and waveguides are explained in detail. The drawings and block diagrams of the inventions are given to describe the limiters better. The purpose of this invention is to protect receiver front ends and sensitive components in the circuit from HPM pulse. It is claimed that the insertion loss of the waveguide limiter is about 2-4 dB, the limiter provides 60 dB isolation during the operation and the opening time of the device is less than 10 ns. In Chapter 5 of this thesis, this vanadium dioxide limiter for waveguide structure is taken as an example model and it is tried to be realized to verify the statement that vanadium dioxide can be used as an RF limiter.

CHAPTER 3

INVESTIGATION OF LNA SUSCEPTIBILITY TO HPM

Front-door attack is mainly HPM energy coupled through dedicated antenna as described before. As shown in Figure 3-1, a typical receiver system of radar, this energy is firstly passed through an RF filter that is not usually affected from HPM pulse. The second component exposed to this high energy is RF amplifier. At this stage, a low-noise amplifier (LNA) is often placed to amplify the weak signals captured by the antenna. LNA is a sensitive semiconductor device and can be easily damaged from high RF levels. Therefore, the most vulnerable component at the receiver part of the radar systems to this HPM energy is low noise amplifier and also the susceptibility level of the LNA is crucial to determine the destruction threshold level of the radar systems.

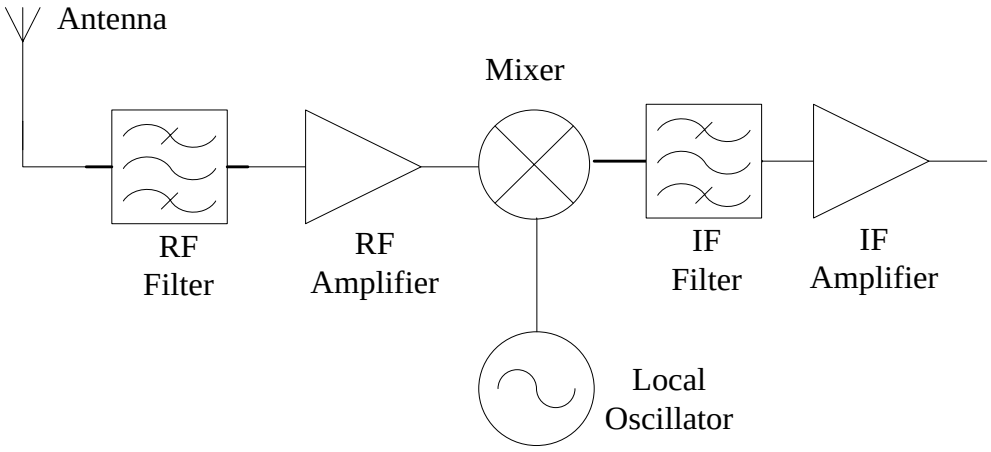

Figure 3-1 : Typical Block Diagram of a Radar Receiver System

In this chapter, a typical military LNA is chosen as a sample and HPM pulses are injected to this device. The investigated sample is chosen to represent the general

LNA technology, and thus, it will give an approximate general picture of the destruction susceptibility levels. The investigations are performed by measuring the gain and supply current of the sample both before and after the injection of HPM pulses of different pulse widths. At a certain threshold voltage, a permanent damage to the LNA is expected to occur. In this chapter, the first experiment is to test this LNA by only one 100 ns pulse with different amplitudes to observe the effects of a short HPM attack. Then, during the next experiment, the characteristics of the pulse are systematically changed in order to figure out the critical levels of the two significant quantities; amplitude and pulse width. After this study, the critical levels of these quantities are determined. The RF pulses above these critical levels damage the chosen LNA.

3.1. LNA Selection

The first step is to choose a typical LNA that represents the general LNA technology and this LNA is used as the sample during the whole study. With the help of this selected LNA, a more general knowledge can be obtained about the performance of the LNA technology against HPM pulse. Gain and noise figure are mostly taken into account during this selection as they are the most important parameters for a LNA used at the first stage of receiver systems. Also, operating frequency is another significant point. In this study, the experiments are carried out at 10 GHz. HMC565LC5 is decided to be used along this experiment since it features 21 dB of small signal gain and 2.5 dB noise figure from 6 to 20 GHz. Moreover, the HMC565LC5 is a high dynamic range GaAs PHEMT MMIC LNA housed in a leadless RoHS compliant 5x5 mm SMT package. This self-biased LNA is ideal for general applications due to its single +3V supply operation and DC blocked RF input and output. Also, the other important parameters of the HMC565LC5 are shown in Table 3-1.

Table 3-1 : Significant Parameters of HMC565LC5 taken from datasheet

Parameter	Min.	Typ.	Max.	Min.	Typ.	Max.	Units
Frequency Range		6 - 12			12 - 20		GHz
Gain	19	21		16	18.5		dB
Gain Variation Over Temperature		0.025	0.035		0.025	0.035	dB/ °C
Noise Figure		2.5	2.8		2.5	3	dB
Input Return Loss		15			12		dB
Output Return Loss		13			15		dB
Output Power for 1 dB Compression (P1dB)	8	10		9	11		dBm
Saturated Output Power (Psat)		11			13		dBm
Output Third Order Intercept (IP3)		20			21		dBm
Total Supply Current (Idd)(Vdd = +3V)		53	75		53	75	mA

3.2. LNA Destruction

The main aim of this study is to investigate whether only one 100 ns pulse can burn an LNA or not. After it is succeeded, another important data obtained from the study is the approximate amplitude of the damaging pulse. For these purposes, two LNA samples are worked on and both of them are burned at the end of the experiment.

First of all, the list of equipments used during the whole experiment is given at the Table 3-2 that also shows manufacturer number, manufacturer and the next date of calibration.

Table 3-2 : List of equipments used in the experiment

Device	Manufacturer Number	Manufacturer	Next Date of Calibration
Power Supply	E3631A	Agilent	05.12.2014
Power Supply	E3631A	Agilent	02.04.2015
Arbitrary Function Generator	33250A	Agilent	13.03.2014
Peak Power Analyzer	4500B	Boonton	24.11.2013
Analog Signal Generator	E8257D	Agilent	11.08.2013
Power Amplifier	-	Aselsan	-
Limiter	TGL2201	Triquint Semiconductor	-
Digital Phosphor Oscilloscope	DPO4104	Tektronix	14.02.2014
Power Detector	202A	Krytar	-
Digital Serial Analyzer	DSA71604	Tektronix	25.07.2013

3.2.1. Experimental Setups

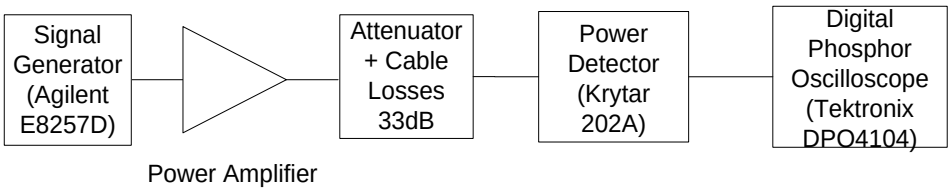

Figure 3-2 : Experimental Setup to check output signal of PA

The purpose of the experimental setup given in Figure 3-2 is to check the amplitude and pulse width of the produced pulse before it is sent to the LNA. Firstly, a 100 ns pulse waveform is sent to the drain input of PA from Arbitrary Function Generator and at this condition, a RF pulse is generated by this system. Then, the pulse amplitude is adjusted by changing signal amplitude of the Signal Generator.

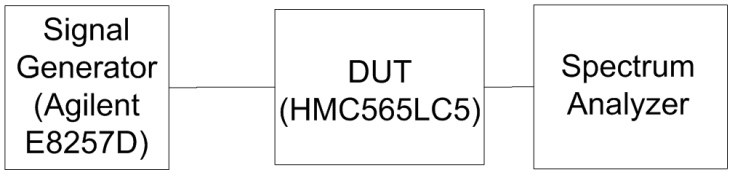

Figure 3-3 : Measurement Setup to control gain of LNA

Before this generated pulse is sent, gain and supply current of the LNA are recorded by using the experimental setup shown in Figure 3-3. In order to observe any instantaneous changes during the experiment, this test is repeated after every sent pulse.

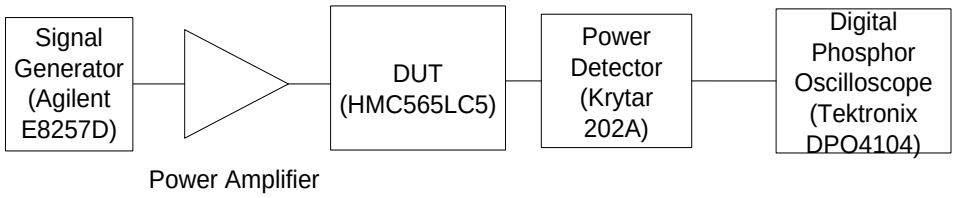

Figure 3-4 : Experimental setup that sends HPM pulses to LNA

The equipments shown in Figure 3-4 are put together and the controlled pulse is sent to DUT. If the DUT is not burned or malfunctioned after this pulse, another pulse with higher amplitude is sent again. This procedure carries on until the gain or supply current of the LNA are significantly changed. Also, the residual pulse after the LNA is always measured to be sure that only one pulse is sent to DUT.

3.2.2. Measurement Results

Table 3-3 summarizes the findings of the tests performed on the first LNA. In this table, the first column gives input signal amplitude of the PA while the second and third ones show gain and supply current of the LNA after the pulse is applied.

Table 3-3 : Test results of the first LNA

Input Signal Amplitude (dBm)	Gain of the LNA (dB)	Supply Current of the LNA (mA)
-5	21	58
0	21	58
5	21	58
10	21	58
11	21	58
12	21	58
13	11	75

As the input signal amplitude of the PA is set to 13 dBm, gain of the LNA decreases and supply current of the LNA increases dramatically. At this step, it is succeeded that the first LNA is burned due to this pulse. Meanwhile, the output of PA is measured with the experimental setup given in Figure 3-2 and the necessary pulse to burn the LNA is shown in Figure 3-5. The amplitude of the pulse is nearly 37.5 dBm but this value is not so accurate due to measurement equipments (power detector and oscilloscope).

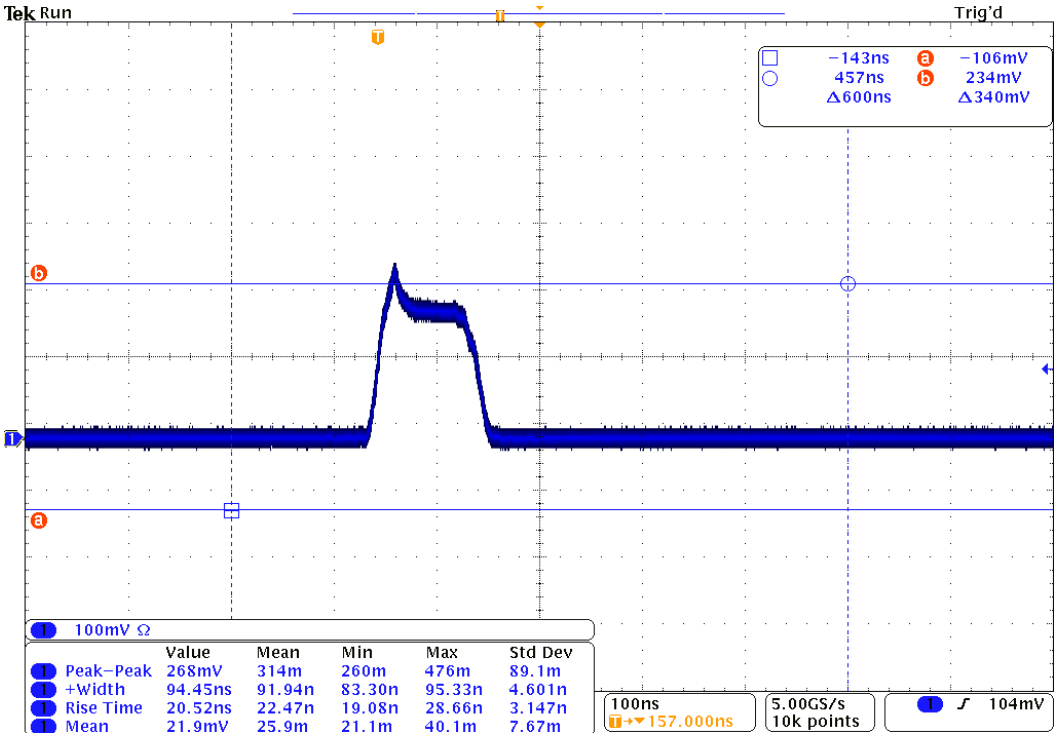

Figure 3-5 : Voltage vs. time graph of measured RF pulse that burns the first LNA

Table 3-4 shows the results of the tests performed in the same manner on the second LNA. At this table, the columns show the same quantities as the previous table.

Table 3-4 : Test results of the second LNA

Input Signal Amplitude (dBm)	Gain of the LNA (dB)	Supply Current of the LNA (mA)
-5	21.2	53
0	21.2	53
5	21.2	53
10	21.2	53
11	21.2	53
12	21.2	53
13	21.2	53
14	15	65

As amplitude of the input signal is set to 14 dBm in this experiment, gain of the LNA and supply current of the LNA begin to change sharply. By looking these inspections, it can be said that the second LNA is damaged from this pulse. The amplitude of the needed pulse to burn the LNA is nearly 38.5 dBm in this case.

In conclusion, the experiments are performed by measuring the gain and supply current of the sample both before and after the injection of HPM pulses of a certain pulse widths, 92 ns. When the results of the experiments from two LNA samples are evaluated, only one HPM pulse whose pulse width is about 100 ns is enough to burn or damage an LNA permanently. Although the amplitude of pulse is not the first consideration in this study, the amplitude of the required pulse is about 38 dBm (6.3 W).

3.3. Effects of Amplitude and Energy on Destruction of LNA

In the preliminary study, it is proved that only one HPM pulse with determined amplitude and pulse width can damage an LNA permanently. The significant parameters of this study are certainly amplitude and pulse width of the HPM pulse. At this stage, the effects of amplitude and pulse width of the pulse on the damage of the LNA are focused on. For this purpose, the pulses with different pulse widths and amplitudes are injected to the LNA to determine the threshold levels of these quantities. At the end of the experiment, it will be clear that amplitude or energy of the pulse is more effective at the destruction of the LNA technology.

3.3.1. Characteristics of Produced Pulse

First of all, the characteristics of the pulse are introduced and determined in order to figure out the threshold points and simulate different front door attacks. Therefore, in the time of this experiment, pulse width is decided to set at three different values: 100 ns, 200 ns and 400 ns which are in the range of HPM pulses (20 ns – 1 μs) [2]. Although HPM pulses can be repetitive as mentioned before,

only one pulse is sent to the LNA in the experiment again. Also, amplitude of the pulse is changed during the experiment so that the critical levels of pulse amplitude can be defined.

3.3.2. Experimental Setups

In order to observe the produced pulse and apply to the LNA, two experimental setups are constructed. The block diagrams and general views of the experimental setups are given in Figure 3-6 and Figure 3-7.

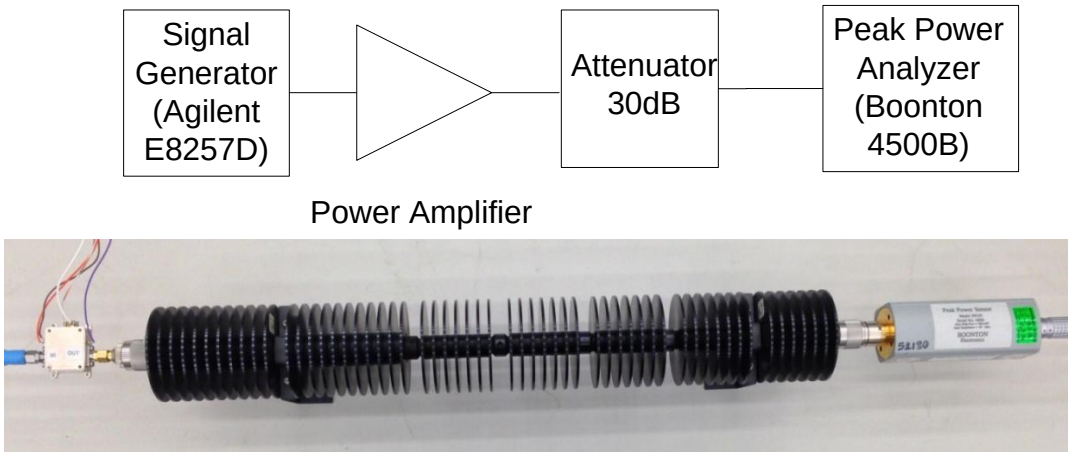

Figure 3-6 : Block diagram and general view of measurement setup to check the produced pulse

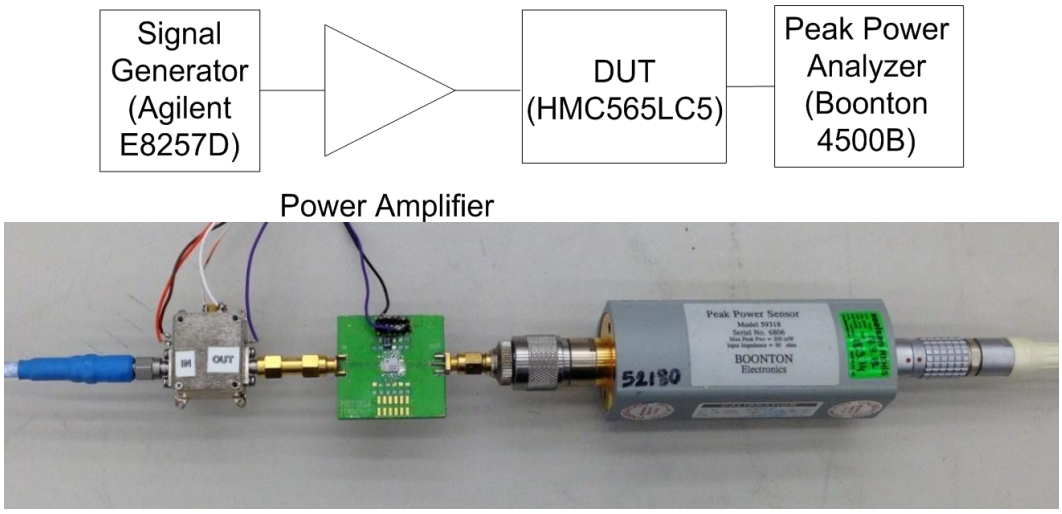

Figure 3-7 : Block diagram and general view of measurement setup to apply HPM pulses

The HPM signal is generated from a power amplifier which is triggered by a waveform generator and input of this power amplifier is produced by a signal generator. Also, the power amplifier needs 3 different voltages; namely -5V, +5V and +9V. In order to produce the desired pulse, firstly -5V is applied to the gate of the PA. After +5V and +9V are turned on, a TTL control input is expected to switch on the amplifier. Then, the PA is ready for the amplification. Gain of this power amplifier is about 21 dB in the saturation region and power amplifier has a maximum output power of 10 W. When the input of the PA is about 19 dBm, the PA can produce an RF signal whose amplitude is nearly 40 dBm. In this experiment, the amplitude of HPM pulse is adjusted by changing the RF signal produced by the signal generator. The output of the PA is measured at the first experimental setup to be sure the amplitude of the pulse before applied to the DUT when the amplitude of the signal generator is altered. This setup is shown in Figure 3-6. In this setup, after PA, the amplitude of the RF signal is too high to be measured by Boonton 4500B. Therefore, some attenuation is necessary to decrease the amplitude of the microwave pulse. For this purpose, a 30 dB attenuator is connected and then, the total attenuation with connector losses is 32.7 dB. After the attenuator, the HPM pulse is measured by the Boonton's peak power analyzer. At this stage, it is guaranteed that HPM pulse is produced with desired amplitude.

The second experimental set-up which is shown in Figure 3-7 is constructed to apply this pulse to the LNA. Up to PA, the configuration is same as the first set-up. After PA, the microwave pulse is injected into device under test (DUT) which is the selected LNA (HMC565LC5) and then DUT is controlled in order to understand that this pulse has caused any damage. Thus, a third set-up is needed to check the LNA whether working properly or not. The control parameters are simply gain and supply current of the LNA, again. A signal generator and a peak power analyzer are enough to check these control parameters. Figure 3-8 gives the block diagram and general view of the control setup.

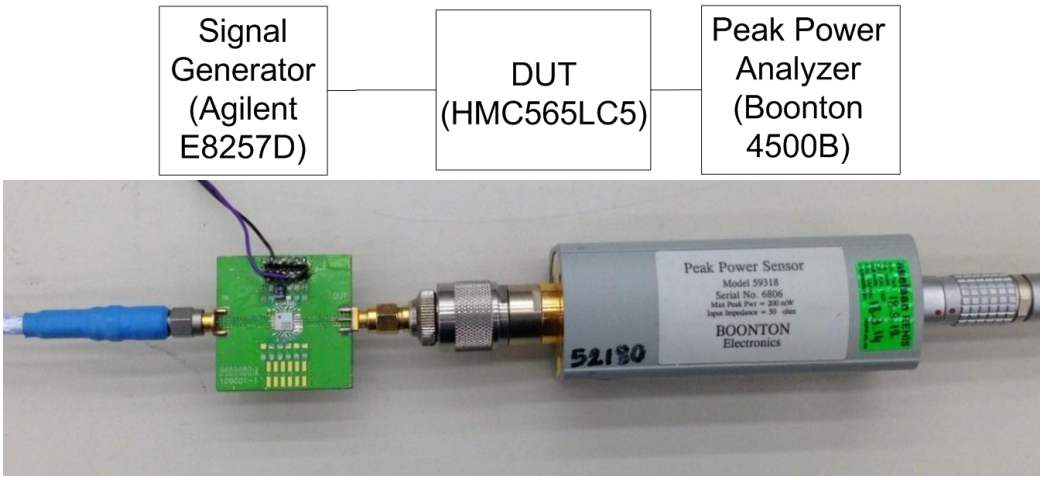

Figure 3-8 : Block diagram and general view of control setup

After the output power of the amplifier is guaranteed by using the peak power analyzer, this power is then applied to the DUT. If LNA is not broken or malfunctioned after the pulse, this procedure is repeated by increasing the output power gradually. When it is succeeded that the DUT is not working anymore, the amplitude and pulse width of the pulse are recorded and also shape of the pulse is saved.

In this stage of experiment, the pulse width is set to 100 ns, 200 ns and 400 ns, respectively and in the beginning of each turn, the amplitude is adjusted to a safety value that is determined by considering the results of preliminary work and it is increased gradually until the destruction. Also, the general procedure to obtain the

destruction threshold levels of LNA is summarized in the flowchart given in Figure 3-9.

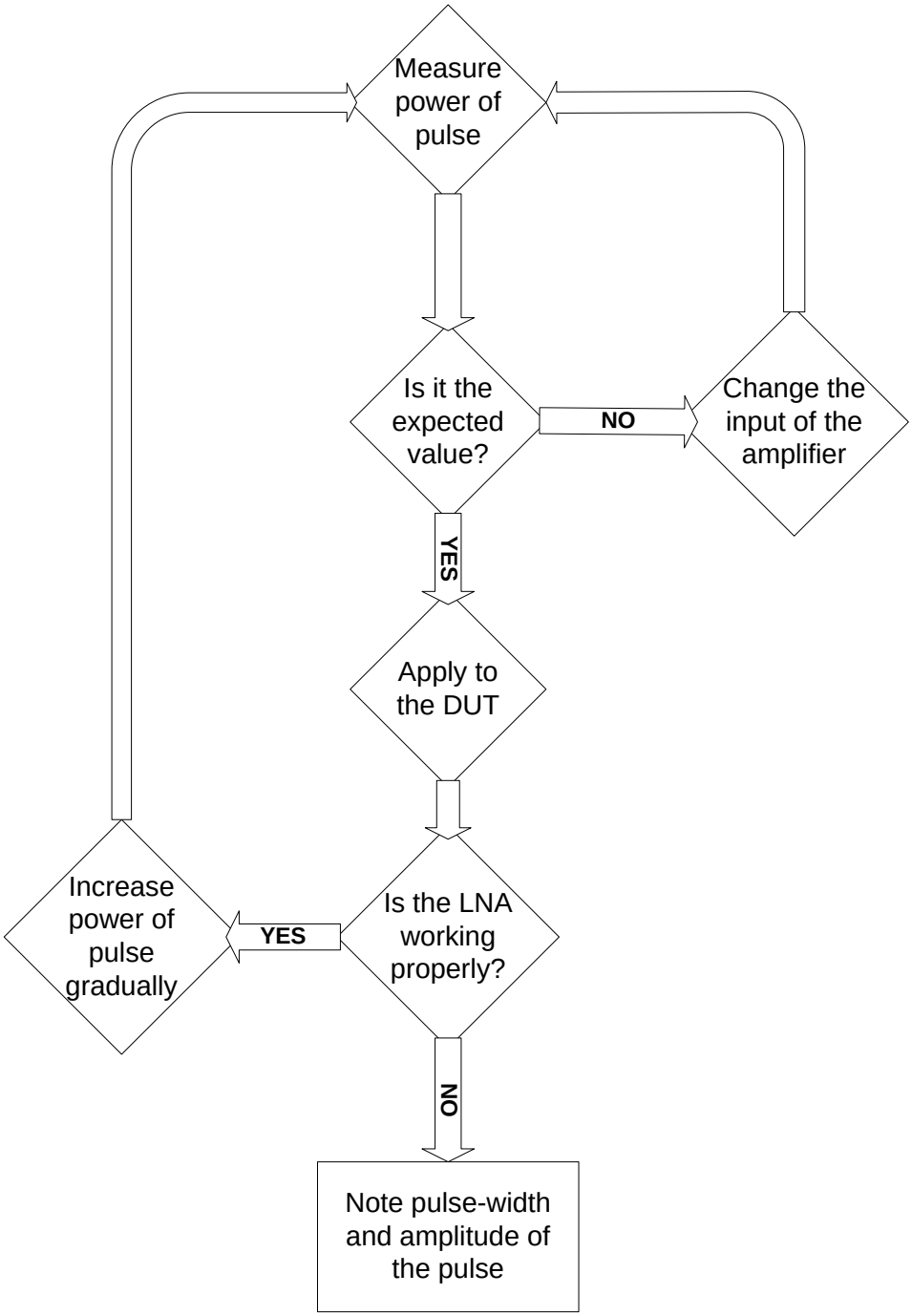

Figure 3-9 : LNA destruction flowchart

3.3.3. Measurement Results

Table 3-5, Table 3-6, Table 3-7, Table 3-8, Table 3-9 and Table 3-10 show the applied power, gain and supply current of the LNA up to the threshold levels of the pulse amplitude for three different pulse widths. When the amplitudes reach to the last value given the tables, the destructions of the DUT occur in each case.

Pulse width=100 ns

Table 3-5 : Test results of the first LNA sample

Applied Power to DUT (dBm)	Gain of the LNA (dB)	Supply Current of the LNA (mA)
37	21.6	59
38	21.6	59
39	18.7	54

Critical Amplitude=39 dBm

Table 3-6 : Test results of the second LNA sample

Applied Power to DUT (dBm)	Gain of the LNA (dB)	Supply Current of the LNA (mA)
37	21.6	59
38	21.6	59
39	18.7	54

Critical Amplitude=39 dBm

Figure 3-10 demonstrates the applied 100 ns RF pulse that causes damage on DUT for both cases. The power shown in this figure is 6.32 dBm. When 32.7 dB attenuation is taken into account, the total power is desired one, 39 dBm.

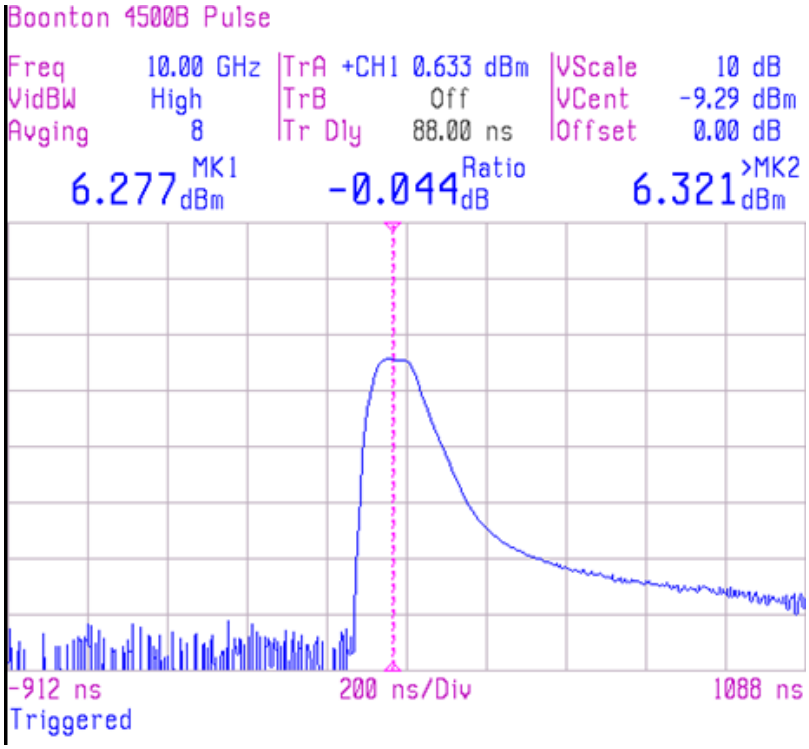

Figure 3-10 : Power vs. time graph of 100 ns pulse that burns both DUTs

Pulse width=200 ns

Table 3-7 : Test results of the first LNA

Applied Power to DUT (dBm)	Gain of the LNA (dB)	Supply Current of the LNA (mA)
34	21.6	55
35	21.6	55
36	21.6	55
37	21.6	55
37.5	21.6	55
38	21.6	55
38.5	21.6	55
39	8.6	84

Critical Amplitude=39 dBm

Table 3-8 : Test results of the second LNA

Applied Power to DUT (dBm)	Gain of the LNA (dB)	Supply Current of the LNA (mA)
38	21.5	61
38.5	21.5	61
39	21.5	61
39.5	18.6	65

Critical Amplitude=39.5 dBm

Figure 3-11 and Figure 3-12 are the screen views of peak power analyzer when the damaging pulses are measured with 32.7 dB attenuation for sample 1 and sample 2, respectively.

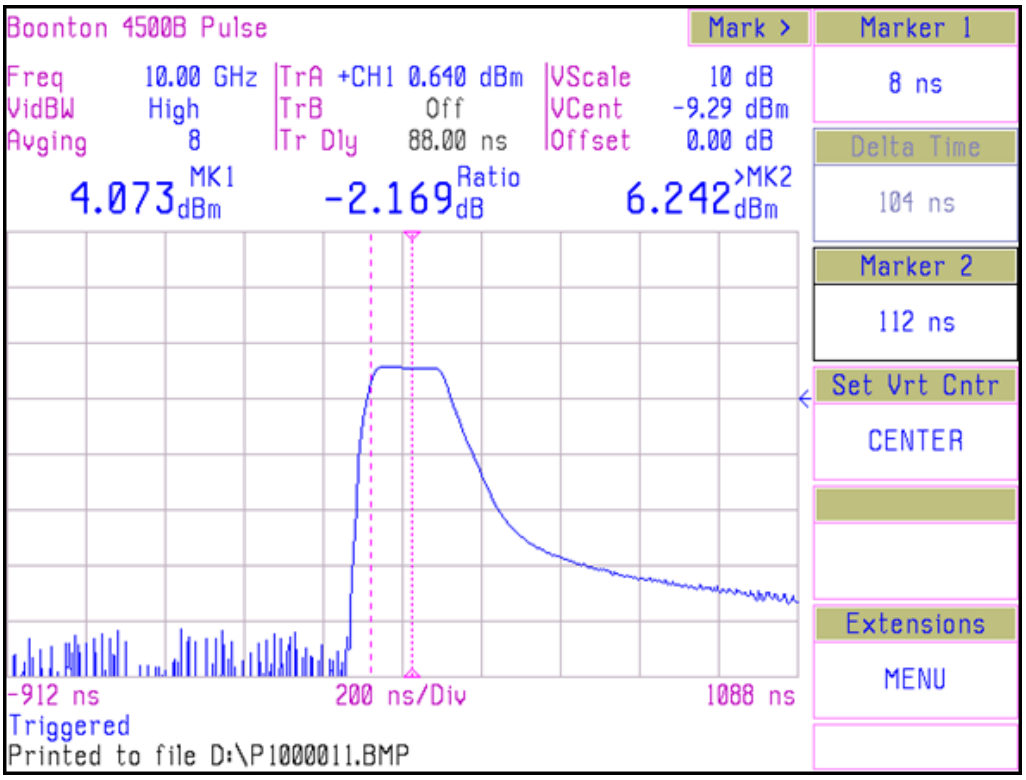

Figure 3-11 : Power vs. time graph of 200 ns pulse that damages the first LNA

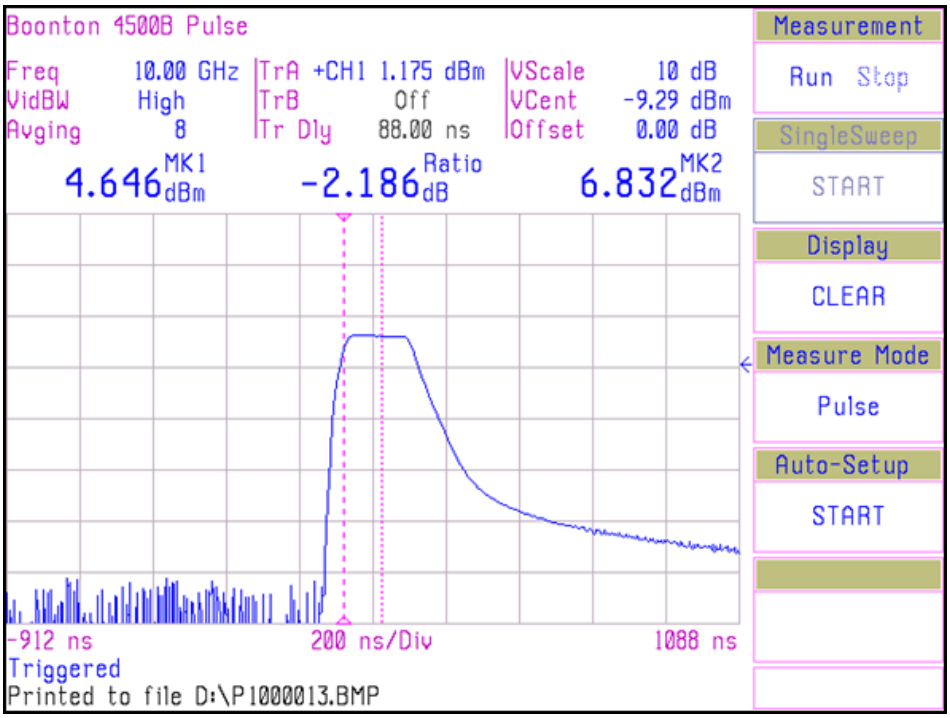

Figure 3-12 : Power vs. time graph of 200 ns pulse that damages the second LNA

Pulse width=400 ns

Table 3-9 : Test results of the first LNA

Applied Power to DUT (dBm)	Gain of the LNA (dB)	Supply Current of the LNA (mA)
37	21.1	60
38	20	61

Critical Amplitude=38 dBm

Table 3-10 : Test results of the second LNA

Applied Power to DUT (dBm)	Gain of the LNA (dB)	Supply Current of the LNA (mA)
36	20.7	57
37	20.7	57
37.5	20.7	57
38	19.4	60

Critical Amplitude=38 dBm

Also, Figure 3-13 gives the pulse shape of the 400 ns RF pulse while the 32.7 dB attenuation is applied again before the peak power analyzer.

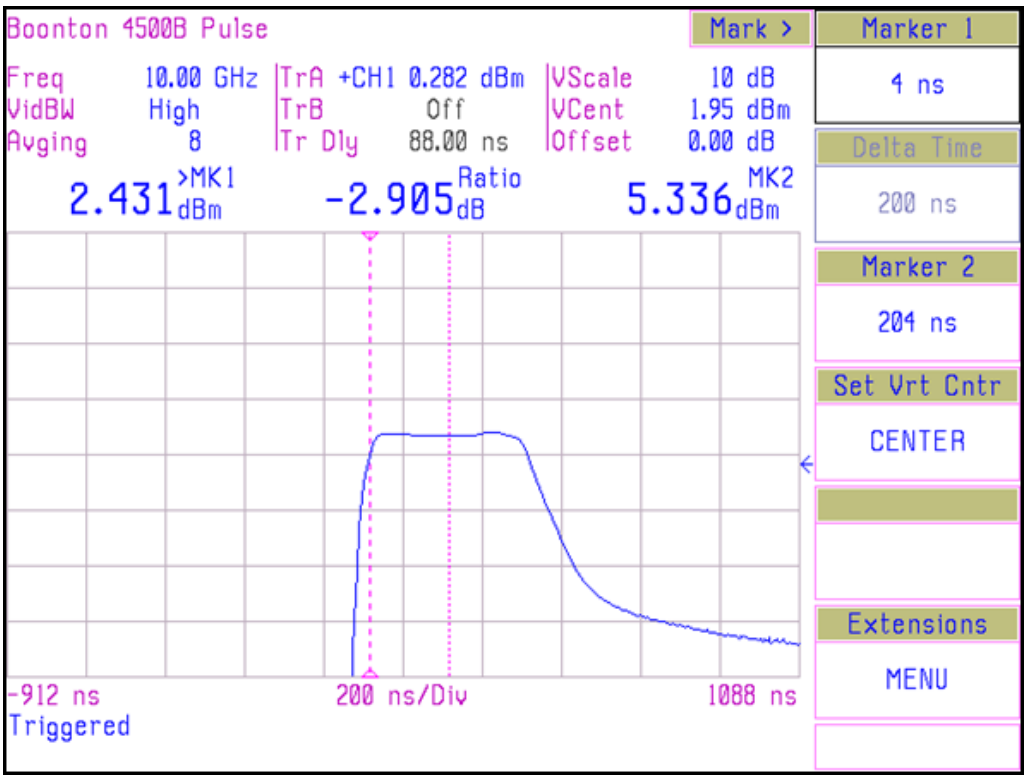

Figure 3-13 : Power vs. time graph of 400 ns pulse that burns both DUTs

In conclusion,

- By using a 100 ns RF pulse with 39 dBm amplitude, 2 LNA samples are burned in the experiment. Thus, the threshold level of pulse amplitude is certainly 39 dBm when pulse width is 100 ns. The used energy to damage the DUT is calculated below:

  Energy = Time X Power =100 ns X 7.94 W = 0.794 uJ

- When pulse width is increased to 200 ns, a 39 dBm pulse and a 39.5 dBm pulse are managed to burn the LNAs. Therefore, the threshold amplitude can be determined as 39 dBm, again. If it is desired to calculate the energy, it is about 1.6 uJ

  Energy = Time X Power =200 ns X 7.94 W = 1.588 uJ

- In the last case, a 400 ns pulse is injected to DUT and when the power amplitude reaches to 38 dBm, both samples are out of use. The energy transferred to DUT during the destruction is:

  Energy = Time X Power =400 ns X 6.31 W = 2.524 uJ

Table 3-11 : Destruction threshold levels, power and energy for LNA for direct injection of HPM pulses of different pulse widths

HPM at f=10 GHz		
Pulse width (ns)	Power(W)	Energy(uJ)
100	7.94	0.794
200	7.94	1.588
400	6.31	2.524

When the destruction threshold levels for direct injection of HPM pulses of 100 ns and 200 ns pulse widths are evaluated, it is obvious that if amplitude of the power reaches 39 dBm (7.94 W), the destruction of LNA occurs independent of applied energy. Also, the power amplitude of 400 ns pulse is close to this value although it is not exactly the same.

On the other hand, when the energy levels of these three states given in Table 3-11 are compared, it is seen that there is no direct relation between applied energy and destruction of DUT.

Thus, it is clear that amplitude of the pulse is more effective at the destruction of the LNA technology and the limiter designed or chosen against HPM should limit HPM pulse before it reaches the power of 39 dBm.

Table 3-12 : Destruction threshold levels, power and energy for LNA for direct injection of HPM pulses of different pulse widths [15]

HPM at f=6 GHz		
Pulse width (us)	Power(W)	Energy(uJ)
0.1	5	0.5
1	2.5	2.5
10	2.5	25

Similar study on a different LNA at 6 GHz is presented in [16]. According to this paper, the destruction threshold level for direct injection of HPM pulse of 100 ns pulse width is determined as 37 dBm (5 W). This threshold level is close to the experimentally obtained results in this chapter although DUT and operating frequency are different. Thus, it is obvious from these two studies, the destruction threshold level of LNA technology is about 39 dBm. Also, when Table 3-12 is evaluated, the destruction of LNA mostly depends on the amplitude level of the HPM as claimed before.

CHAPTER 4

INVESTIGATION OF DIODE LIMITER STRUCTURES

In this chapter, two limiter structures based on diode technology are investigated against HPM pulses in terms of power handling capacity and response time. Firstly, a diode limiter which is commercially available in the market is tested under a high power microwave pulse to figure out the characteristics of diode limiter technology against this threat. Moreover, the limits of this device in terms of response time and leakage output power are examined for this purpose. Secondly, a high power PIN diode is focused on and the approximate response time of the limiter is obtained by using the specifications in the datasheet and making some interpretations.

The block diagram of a dual stage diode limiter is shown in Figure 4-1. Basically, it consists of four diodes and only two of them are active simultaneously. In other words, two diodes are active and clip large signals at positive cycles of the RF signal whereas the others are active at negative cycles of the signal to limit high power microwave signals.

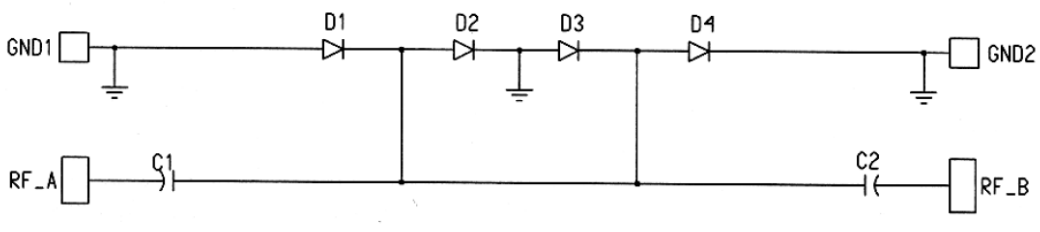

Figure 4-1 : Detailed block diagram of TGL2201, a dual stage diode limiter

For this test, TGL2201 that is a wideband dual stage VPIN limiter from Triquint Semiconductor is chosen due to some significant features given below:

Features:

- 3-25 GHz Passive, High Isolation Limiter
- Low Loss < 0.5 dB at X-band
- Good Return Loss > 15 dB
- Flat Leakage < 18 dBm
- Input Power CW Survivability < 5 W
- Integrated DC Block on both input and output

Table 4-1 : Maximum ratings of TGL2201

Symbol	Parameter 1/	Value
P_{IN}	Input Continuous Wave Power	37 dBm
T_M	Mounting Temperature (30 Seconds)	320 ^{0}C
T_{STG}	Storage Temperature	-65 to 150 ^{0}C

Table 4-2 : RF characteristics of TGL2201 at 25°C

Symbol	Parameter	Test Condition	Limit			Units
			Min	Typ	Max	
IL	Insertion Loss	F = 4-20 GHz	--	0.5	1.0	dB
IRL	Input Return Loss	F = 4-20 GHz	12	--	--	dB
ORL	Output Return Loss	F = 4-20 GHz	12	--	--	dB
PWR	Output Power @ P_{in} = 27 dBm	F = 6.0 GHz F = 16.0 GHz	-- --	-- --	20 20	dBm dBm

The maximum ratings and RF characteristics of the device that are mostly suitable to the purpose of this study are shown in Table 4-1 and Table 4-2, respectively. In Table 4-2, it is stated that the limiter works at 10 GHz which is the operating frequency of the experiment and output power is 20 dBm which is not a dangerous level for LNA technology. However, according to Table 4-1, the maximum input continuous wave power is given as 37 dBm (5 W). In this experiment, a HPM pulse above the maximum input power is applied and performance of the device under HPM attack is observed.

In this test, a HPM pulse is produced by using the power amplifier used in chapter 3. Then, this pulse is sent to the selected limiter to observe the characteristics of the limiter and also, the residual pulse is measured to obtain the output leakage power level of the device. First of all, before the produced pulse is applied to the limiter, it is measured again by a high speed oscilloscope (Digital Serial Analyzer) to assure the amplitude and pulse width of the pulse.

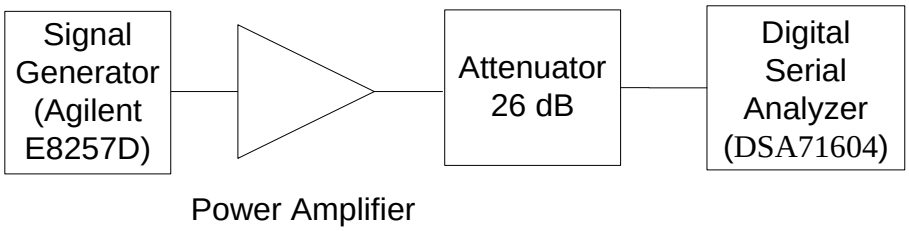

Figure 4-2 : Block diagram of measurement setup to check the produced pulse

The block diagram of the measurement setup is given in Figure 4-2. The amplifier and signal generator (E8257D) are used in order to obtain a HPM pulse. Before the oscilloscope, a 26 dB attenuator is placed to decrease this high RF signal level to a sensible level for the oscilloscope. Next, the measurement is finalized when the desired pulse is obtained and the signal given in Figure 4-3 is obtained.

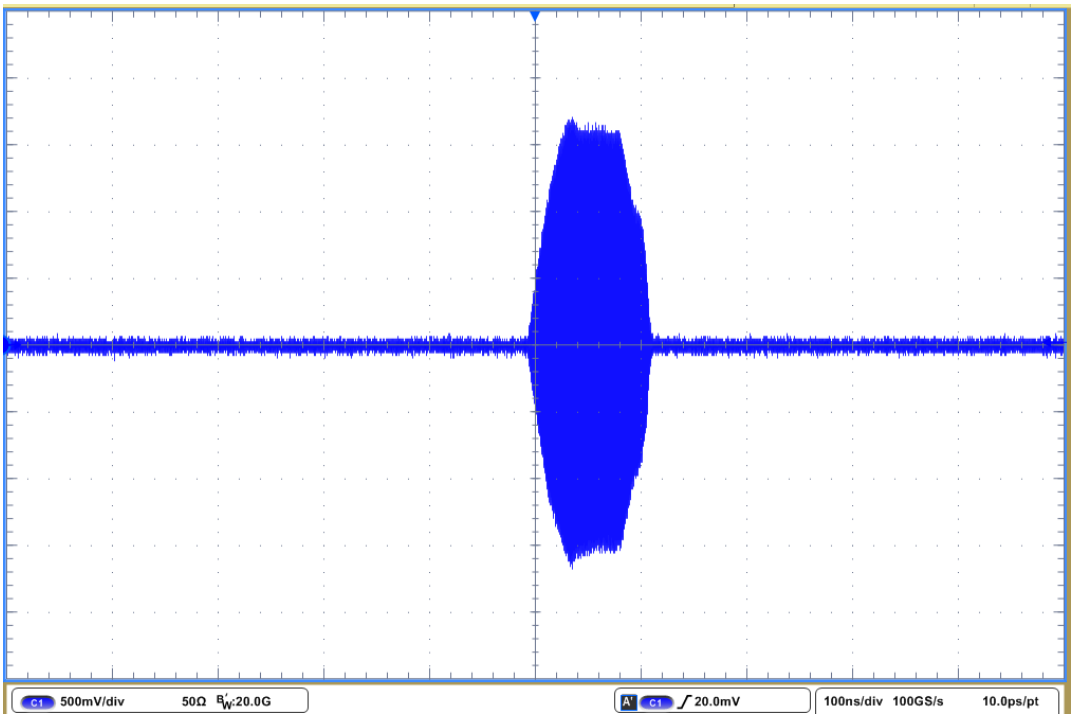

Figure 4-3 : Voltage vs. time graph of desired RF pulse with a 26 dB attenuator

This graph does not illustrate the power of the pulse directly. Instead, it shows the voltage level of the RF signal as an oscilloscope is used for this measurement. By a short calculation, the output power can be reached as shown below:

$$P = \frac{{V_{peak}}^2}{2R} = \frac{1.5^2}{2 \times 50} = 0.0225\ W = 22.5\ mW$$

$$P = 10 \times \log 22.5 = 13.5\ dBm$$

When the attenuation (26 dB) is taken into account, total peak power is:

$$P_{TOTAL} = 13.5 + 26 = 39.5\ dBm$$

Shortly, the peak power of the pulse is calculated as 39.5 dBm (8.9 W). Then, the produced pulse is given to the limiter by using the experimental setup shown in Figure 4-4. In this configuration, after HPM pulse is produced, it is injected to the limiter and the output of the limiter is recorded.

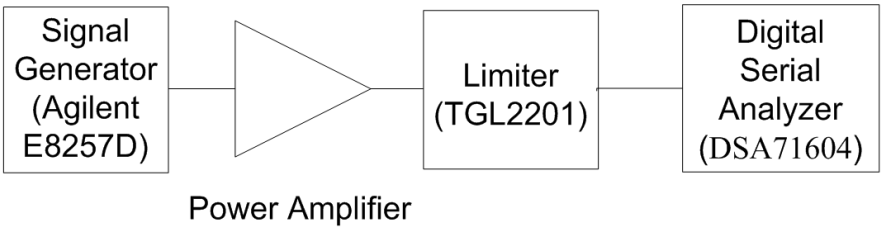

Figure 4-4 : Experimental Setup to apply HPM pulse to limiter

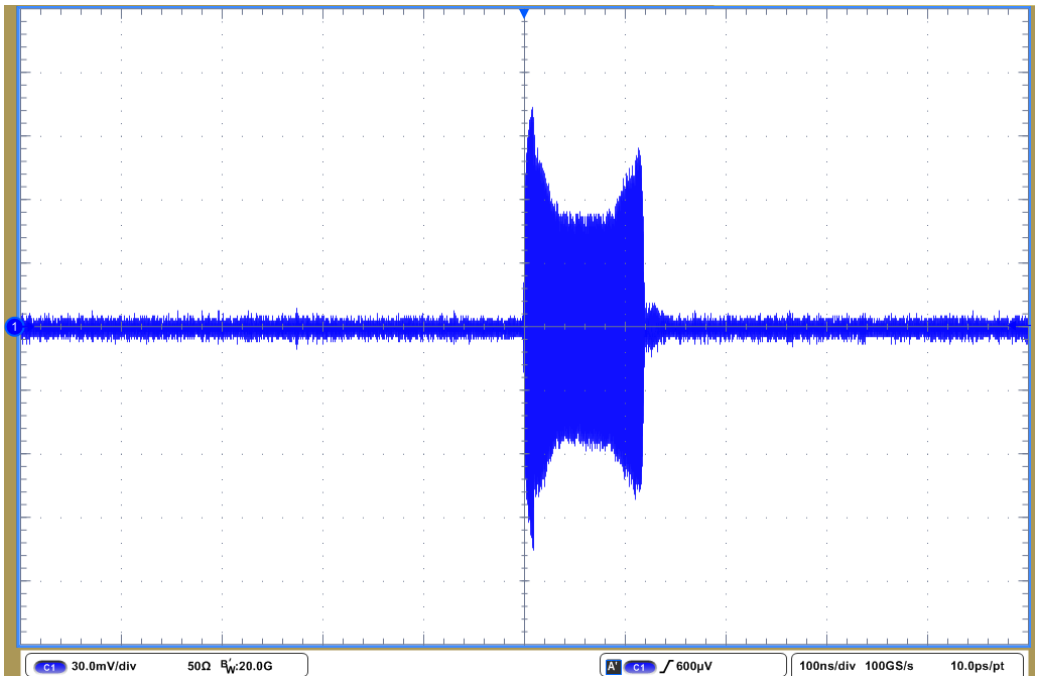

Figure 4-5 : Voltage vs. time graph of leakage pulse of limiter with a 26 dB attenuator

Figure 4-5 shows the output response of the limiter. From this figure, it is seen that the response time of the limiter is about 10 ns which can be defined as a fast response time for a limiter. Again, the peak power can calculated as shown before:

$$P = \frac{{V_{peak}}^2}{2R} = \frac{0.105^2}{2 \times 50} = 0.00011\ W = 0.11\ mW$$

$$P = 10 \times \log 0.11 = -9.5\ dBm$$

When the attenuation (26 dB) is considered, total peak power is:

$P_{TOTAL} = -9.5 + 26 = 16.5\ dBm$

In the previous chapter, it is stated that in order to protect the LNA, the limiter used against HPM threat should limit HPM pulse before it reaches the power of 39 dBm. In this case, the chosen limiter lets the injected RF signal rise up to 16.5 dBm that is maximum leakage power of limiter and then, it begins to limit the RF signal to 12 dBm. This leakage power is not a dangerous level for LNA technology. In conclusion, TGL2201 is a fast and adequate limiter to limit an RF signal whose peak power is up to 40 dBm. However, when the incoming signal is larger, TGL2201 may not be enough for system protection. Also, according to manufacturer, any power higher than 5 W is not safe even the input signal is not a continuous wave (or it is a pulse wave).

For larger amplitude HPM pulses, TGL2201 is not sufficient to protect the sensitive components in the radar system as mentioned before. Therefore, a high power diode is necessary against this HPM threat. A commonly used high power diode, CLA4609, is selected to investigate its protection performance. This chosen diode represents high power silicon diode technology and gives a general idea about the performance of a diode limiter against this type of HPM attack.

CLA4609 is a silicon limiter diode of Skyworks Company. The power handling capacity, the most distinguishing parameter of this product, is 44 dBm for continuous operations as shown in Table 4-4. Also, Figure 4-6 shows the output vs. input power characteristics of CLA4609. Above 40 dBm input power, the diode begins to decrease the output power.

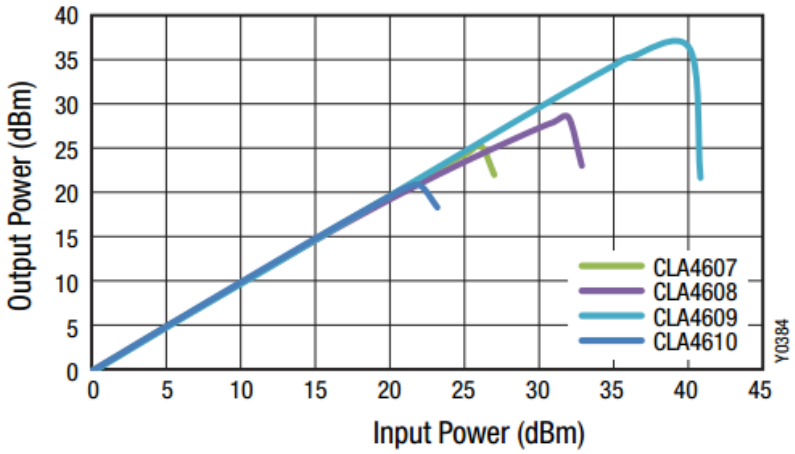

Figure 4-6 : CW output vs. input power of CLA4607 to CLA4610

As it is seen from electrical specifications and typical performances of CLA series diodes given in Table 4-3 and Table 4-4, the power handling capacity or maximum CW input power is directly proportional to the intrinsic region of PIN diode. When the intrinsic regions are compared from CLA4607 to CLA4610, it is obvious that if the intrinsic region is larger, the handled power is also greater as shown in these tables. Not only this CLA series diode example, but also this relation between intrinsic region and power handling capacity is generally valid in PIN diode technology.

Table 4-3 : Electrical specifications of CLA series diodes

Part Number	Breakdown Voltage (V)	I Region (µm)	Junction Capacitance (C_J) @ 0 V (pF)	Junction Capacitance (C_J) @ 6 V (pF)	Series Resistance (Rs) @ 10 mA (Ω)	Minority Carrier Lifetime (T_L) @ 10 mA (ns)	Thermal Resistance (θ) (Note 3)		
							Average (°C/W)	1 µs Pulse 0.1% Duty Cycle (°C/W)	Input Power (W)
	Min to Max	Nominal	Typical	Maximum	Maximum	Typical	Maximum	Typical	Typical
CLA4601-000	15 to 30	1	0.12	0.10	2.5	5	47	47	2.0
CLA4602-000	15 to 30	1	0.20	0.15	2.0	5	59	59	1.7
CLA4603-000	20 to 45	1.5	0.20	0.15	2.0	5	45	45	2.1
CLA4604-000	30 to 60	2.0	0.12	0.10	2.5	7	64	64	1.7
CLA4605-000	30 to 60	2.0	0.20	0.15	2.0	7	53	53	1.6
CLA4606-000	45 to 75	2.5	0.20	0.15	2.0	10	54	54	1.6
CLA4607-000	120 to 180	7.0	0.20	0.15 @ 50 V	2.0	50	91	91	1.0
CLA4608-000	120 to 180	7.0	0.60	0.50 @ 50 V	1.2	100	123	123	1.1
CLA4609-000	250 (Min.)	20	0.26	0.14	1.5	1175	52	52	2.9
CLA4610-000	80 to 120	4.5	0.13	0.12	2.2	20	72	72	1.3

Another crucial parameter for a limiter is response time that is the time from when a pulse hits the limiter until the on-state of limiter is fully activated as described obviously in Figure 4-7.

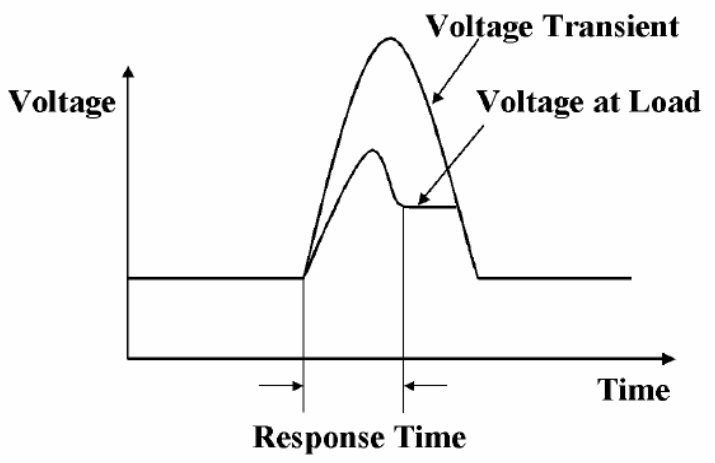

Figure 4-7 : Response time of a typical limiter [2]

PIN diode technology has a finite response time that sometimes affects the performance of the designed system. Also, the wider intrinsic region CLA4609 has is undesired property for response time because in general, the larger intrinsic region of a diode limiter means the longer response time to coming signals. Since the HPM pulses have very short pulse widths, the response or turn-on time of the limiter should be as short as possible so that the system discards this HPM attack without any significant hazard. In other words, if the response time is too long, a large part of the pulse power will pass through the limiter and reach to the sensitive components. Therefore, before this high power PIN diode is used, the response time of the device is also checked from the datasheet if this parameter is short enough or not. When datasheet of CLA4609 is investigated from this point of view, it is seen that the response time of the diode is not given directly. Nevertheless, if the given diode specifications are examined in detail and some basic calculations are done, one can reach some intuitions about response time.

Table 4-4 : Typical Performances of CLA series diodes

Part Number	Insertion Loss @ –10 dBm (dB)	CW Input Power for 1 dB Insertion Loss (dBm)	Maximum CW Input Power (dBm)	Maximum Pulsed Input Power (dBm) (Note 2)	Output @ Maximum Pulsed Input (dBm) (Note 2)	Recovery Time (ns) (Note 3)	Spike Leakage (ergs) (Note 4)
CLA4601-000	0.1	12	36	65	21	5	Note 5
CLA4602-000	0.1	12	36	65	24	5	Note 5
CLA4603-000	0.1	10	38	67	22	5	Note 5
CLA4604-000	0.1	11	40	70	24	5	Note 5
CLA4605-000	0.1	12	40	70	27	5	0.08
CLA4606-000	0.1	14	41	71	27	5	0.03
CLA4607-000	0.1	26	43	73	39	5	0.21
CLA4608-000	0.2	26	43	73	44	5	0.15
CLA4609-000	0.3	37	44	74	50	5	25.77
CLA4610-000	0.1	24	40	57	32	5	Note 5

For this purpose, the specification given in the last column of Table 4-4, spike leakage (ergs), should be interpreted in depth. The spike leakage is commonly measured in ergs and calculated as follows:

$$Spike\ Leakage\ (ergs) = t_s \times P_s \times 10^7$$

where

t_s : the spike width at the half-power point (in seconds),

P_s : the maximum spike amplitude in watts.

These descriptions are represented in Figure 4-8 to be understood clearly. Although the response time of the diode cannot be reached exactly, it can be definitely said that the response time is larger than t_s, the spike width at the half-power point. Then, after the calculation of the spike width, general information about response time of the diode is obtained.

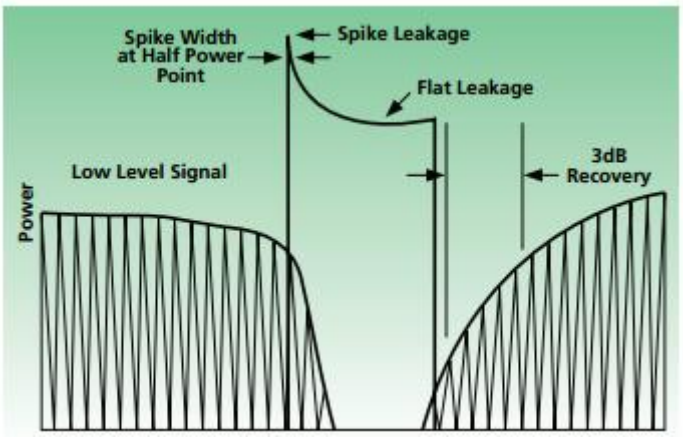

Figure 4-8 : Spike leakage of a typical limiter

The given spike leakage value in datasheet is 25.77 ergs. The maximum spike amplitude (P_s) should be taken as 8 Watts (39 dBm) since the threshold power to burn the chosen LNA is measured as 39 dBm in the previous chapter. Then, according to these values, the spike width is calculated as follows:

$$Spike\ Leakage\ (ergs) = t_s \times P_s \times 10^7$$
$$25.77\ ergs = t_s \times 8 \times 10^7$$
$$t_s = 322.125\ ns$$

From the obtained spike width at the half-power point, it is clear that the response time of CLA4609 is longer than 322 ns if the applied power is about 39 dBm. Therefore, this response time of the diode is too long to challenge a HPM threat. In other words, most of the pulse energy passes this limiter before it completely opens.

In conclusion, TGL2201 and CLA4609 are not suitable solutions to the HPM threat since TGL2201 is not recommended for larger amplitude signals although the turn-on time is measured as 10 ns whereas the response of CLA4609 is too slow to this kind of threats though it can handle high power pulses successfully.

CHAPTER 5

VANADIUM DIOXIDE LIMITER DESIGN

5.1. Vanadium Dioxide Production

In this chapter, firstly, vanadium dioxide (VO_2) is produced in two different ways, namely, with oxalic and formic acids. Then, the synthesized VO_2 is analyzed with X-ray diffraction technique and the temperature-resistance characteristics of VO_2 are investigated by using a multimeter to determine whether these syntheses are successful or not. After it is certain that the material is produced successfully, VO_2 limiter is designed with different dimensions to reach the best design. Finally, insertion losses of these limiters are measured during change of state and then, the design of VO_2 limiter is optimized according to these results.

5.1.1. Syntheses of Vanadium Dioxide

The hydrothermal methods with oxalic acid ($C_2H_2O_4$) and formic acid (HCOOH) are carried out in order to obtain VO_2 samples that are necessary for the design process of the limiter. In these syntheses, Aldrich (NH_4VO_3) is used as precursor or the source of vanadium. Firstly, the synthesis procedure of VO_2 with oxalic acid ($C_2H_2O_4$) is explained step by step below:

- 2.334g NH_4VO_3 is dispersed in 80 ml water and this combination is stirred until all NH_4VO_3 particles are dissolved in the water.

- 3.6g oxalic acid is added to this solution and they are again stirred until the color of this liquid turns to dark blue as seen in Figure 5-1. In [17], it is stated that according to valence of vanadium, the solution can have different colors. For instance, the solution of V^{5+} is yellow whereas this blue color indicates the solution of V^{4+}.
- After 48-hour waiting period, this mixture is put into a reactor shown in Figure 5-1.

Figure 5-1 : Mixture of Oxalic Acid, Water, NH_4VO_3 and Reactor

- This reactor is placed in an oven whose temperature is adjusted to 180°C
- After 48-hour waiting period in this oven, the reactor is taken and cooled at room temperature.
- Then, the solution taken from the reactor is separated by centrifugation. This separation procedure is repeated three times and then dried at 60°C to obtain VO_2 sample in powder form.

The reactions and decompositions during this synthesis process are listed below [17]:

$$2NH_4VO_3 + 4C_2H_2O_4 \rightarrow (NH_4)_2[(VO)_2(C_2O_4)_3] + 2CO_2 + 4H_2O$$

$$(NH_4)_2[(VO)_2(C_2O_4)_3] \rightarrow 2VOC_2O_4 + 2NH_3 + CO + CO_2 + H_2O$$

$$VOC_2O_4 \rightarrow VO_2 + CO + CO_2$$

After the first synthesis of VO_2, the second hydrothermal method to produce VO_2 with formic acid (HCOOH) is introduced in detail:

- 1.2g NH_4VO_3 is put into 50 ml water to obtain a yellow solution and this combination is stirred until all NH_4VO_3 particles are dissolved in the water. In meanwhile, the solution is heated to 50°C in order to make solvation process easier.
- 1.2g formic acid (HCOOH) is added to this solution little by little and they are again mixed until the color of this liquid turns to pink.
- This mixture is put into a reactor and this reactor is placed in an oven whose temperature is adjusted to 180°C again.
- After 48-hour waiting period in this oven, the reactor is taken and opened.
- The solution taken from the reactor is separated by centrifugation method and dried at 60°C to get rid of water. Then, VO_2 particles synthesized by using formic acid are ready for characterization process.

5.1.2. Characterization of Synthesized VO_2 Samples

After syntheses of VO_2 are completed, in order to characterize materials and check the success of syntheses, some parts of these materials are used at X-ray diffraction and investigation of temperature-resistance characteristics of samples.

5.1.2.1. Resistance Characteristics of VO_2 Samples

The produced VO_2 samples are obtained in powder form. Therefore, their resistances cannot be measured with using probes of multimeter in this form. In order to measure them, they are firstly compressed by a compressor to convert into solid form. Then, these solid samples are sticked to two copper wires used to probe from two sides as shown in Figure 5-4. For this process, silver glue is preferred to carry out the continuity of electrical conductivity that is necessary for resistance measurement. After one or two hours, the samples are ready to be measured with a

multimeter. The heater as shown in Figure 5-4 is used to increase the temperature of the VO_2 samples up to 250°C. Meanwhile, at some selected temperatures, the resistance of the samples are measured and recorded. These recorded data is given in Table 5-1 and also these results are given as graphs in Figure 5-2 and Figure 5-3.

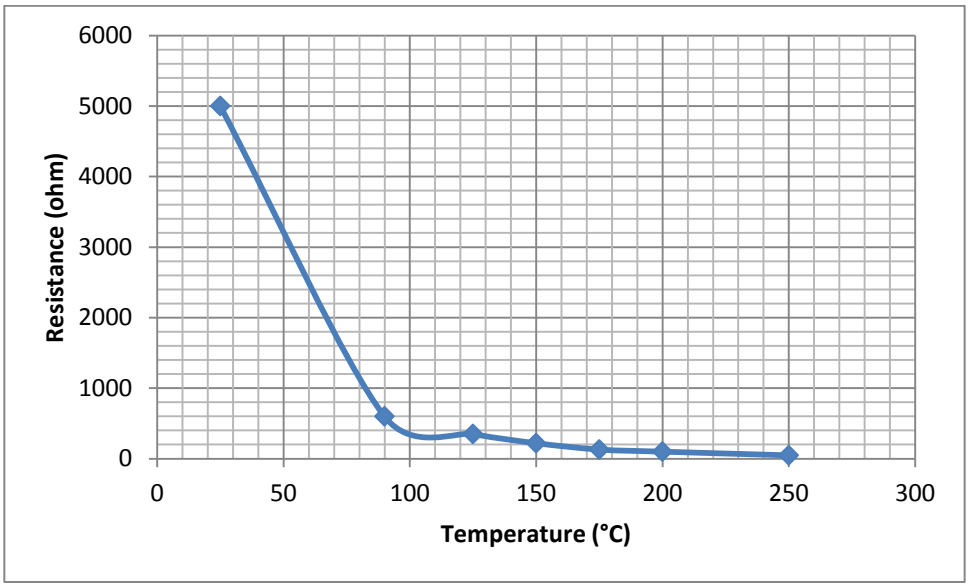

Figure 5-2 : Resistance vs. temperature graph of sample synthesized with oxalic acid

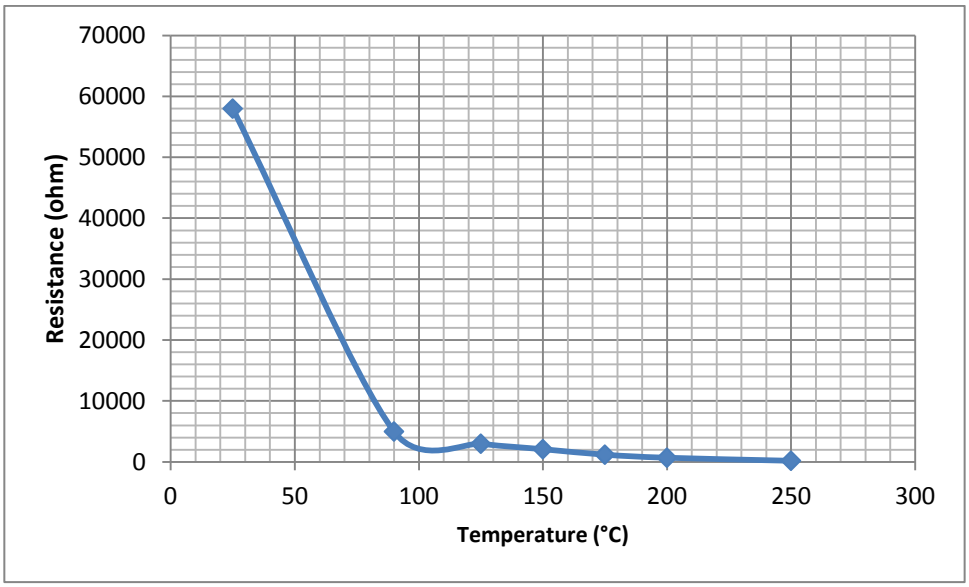

Figure 5-3 : Resistance vs. temperature graph of sample synthesized with formic acid

Table 5-1 : Resistance characteristics of both samples

Temperature	Resistance of Sample 1 (Oxalic Acid)	Resistance of Sample 2 (Formic Acid)
25°C	5kΩ	58kΩ
90°C	600Ω	5kΩ
125°C	350Ω	3kΩ
150°C	220Ω	2.1kΩ
175°C	130Ω	1.2kΩ
200°C	100Ω	700Ω
250°C	48Ω	200Ω

Figure 5-4 : Samples in solid form and heater

When these results are assessed, it is clear that the resistances of both samples decrease while temperatures of materials increase as expected. In other words, these samples behave as an NTC material. Another interesting result of this study is that these two VO_2 samples have different resistance values but the behaviors of them against temperature change are nearly the same as obviously seen in Table 5-1. Also, when the most possible temperatures in real scenario that are 90°C and 125°C are taken into account, the resistances of both samples decrease by 10-20 times. This resistance change is enough to design an RF limiter against HPM pulse.

Also, the insertion loss variations of designed limiter caused by this resistance change will be illustrated in 5.2.5.

However, expected change in the resistivity which is in the order of 10^4 [14] is much higher than the obtained one. Main reasons of this weaker result are divided into two parts. Firstly, the phase of material is converted from powder to solid form by using a basic compressor. This method cannot be guaranteed that the material is totally solid or there is no air gap between the VO_2 particles. These unavoidable air gaps in this method result in discontinuities of electrical conductivity that limit the increase of conductivity. The second reason may be the used VO_2 material in the experiment. If the synthesis of the material is repeated a few times more and made some iterations on the synthesis process, the result can be improved significantly.

5.1.2.2. X-ray Diffractions of VO_2 Samples

This technique is applied to produced samples in order to obtain the crystalline contents of materials. Figure 5-5 and Figure 5-6 illustrate XRD patterns of VO_2 samples produced with oxalic and formic acids, respectively. In the first figure, nearly all peaks of the sample produced with oxalic acid show a typical crystalline structure of the metastable VO_2 with a monoclinic phase. There are few unidentified peaks in this pattern which indicates that the purity of the sample is high. The result of this sample is also compatible with the XRD pattern of VO_2 given in [18]. Moreover, this crystalline structure is coherent with the standard value of JCPDS NO. 31-1438. On the other hand, XRD spectrum of the second sample does not matched with any standard XRD pattern. This spectrum mostly corresponds to combination of monoclinic VO_2 phase [18] and metastable VO_2 phase [9],[19]. Therefore, two different phases of VO_2 exist in the sample produced with formic acid. Also, there are some unexpected peaks in this result which shows the purity of the material, again. In conclusion, according to these XRD patterns, it can be said that these two VO_2 samples are successfully synthesized with hydrothermal methods.

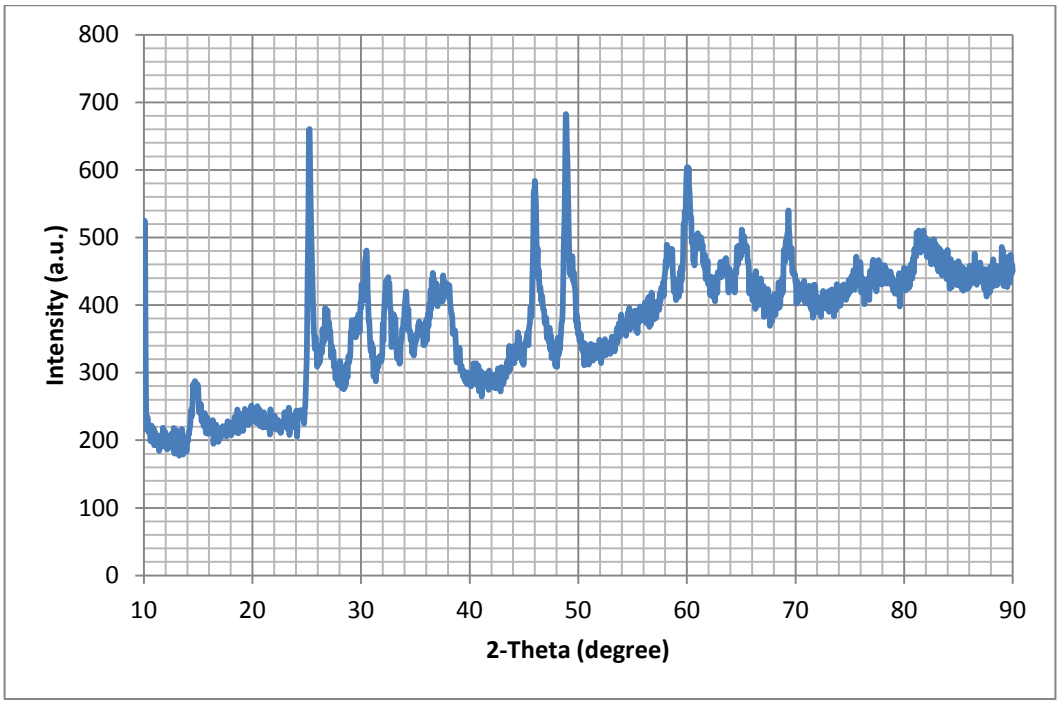

Figure 5-5 : XRD pattern of VO_2 sample produced with oxalic acid

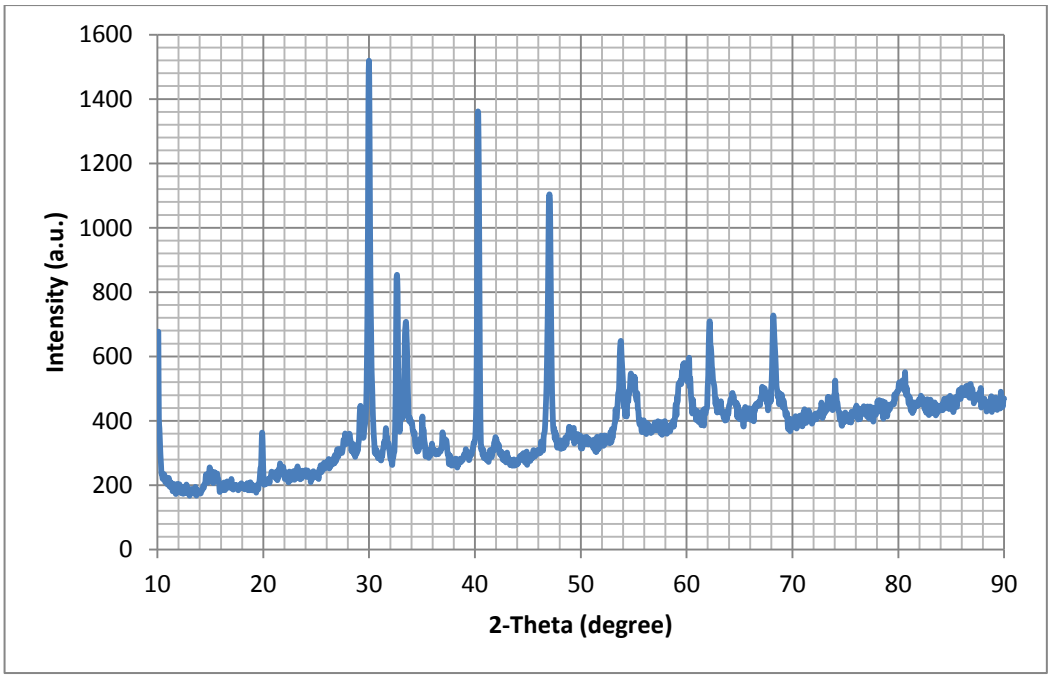

Figure 5-6 : XRD pattern of VO_2 sample produced with formic acid

5.2. Limiter Design

Syntheses and characterizations of VO_2 samples are completed successfully. Now, it is time to design the VO_2 limiter by using these samples. This limiter can be designed for two different structures namely; coaxial cable and waveguide. In [3], two example structures for this purpose are introduced in detail. The drawings of these limiters are given in Figure 5-7.

5.2.1. Design Examples for Coaxial Cable and Waveguide

The working principles of these shown designs proposed in [3] are explained below:

In the limiter suitable for coaxial cable, RF signal is carried by a rod that passes through a circular plate. This plate mainly consists of conductive rings and VO_2 rings. The operating mechanism of the limiter is very simple and straightforward. When VO_2 rings are activated by coming HPM pulses, the VO_2 rings are turned to conductive state and then, the circular plate becomes totally a conductor. Therefore, this conductor reflects RF signal and does not allow passing through the limiter. Otherwise, VO_2 rings behave as an insulator layer between RF signal and ground so RF signal passes the limiter without any significant loss. The threshold level of limiter and the maximum power handling can be optimized in this system by changing the number of VO_2 rings on the plate and number of plates on the line.

The second limiter is placed into a WR90 waveguide. In this structure, most part of the limiter is conductive and only a strip in the middle of the limiter is transition material or VO_2 in this thesis. When HPM pulses activate the VO_2 strip, the plate behaves like a reflector and all of the HPM pulses are turned back in theory. On the other hand, while the VO_2 strip is an insulating layer, this plate forms a capacitive iris which causes only a small attenuation.

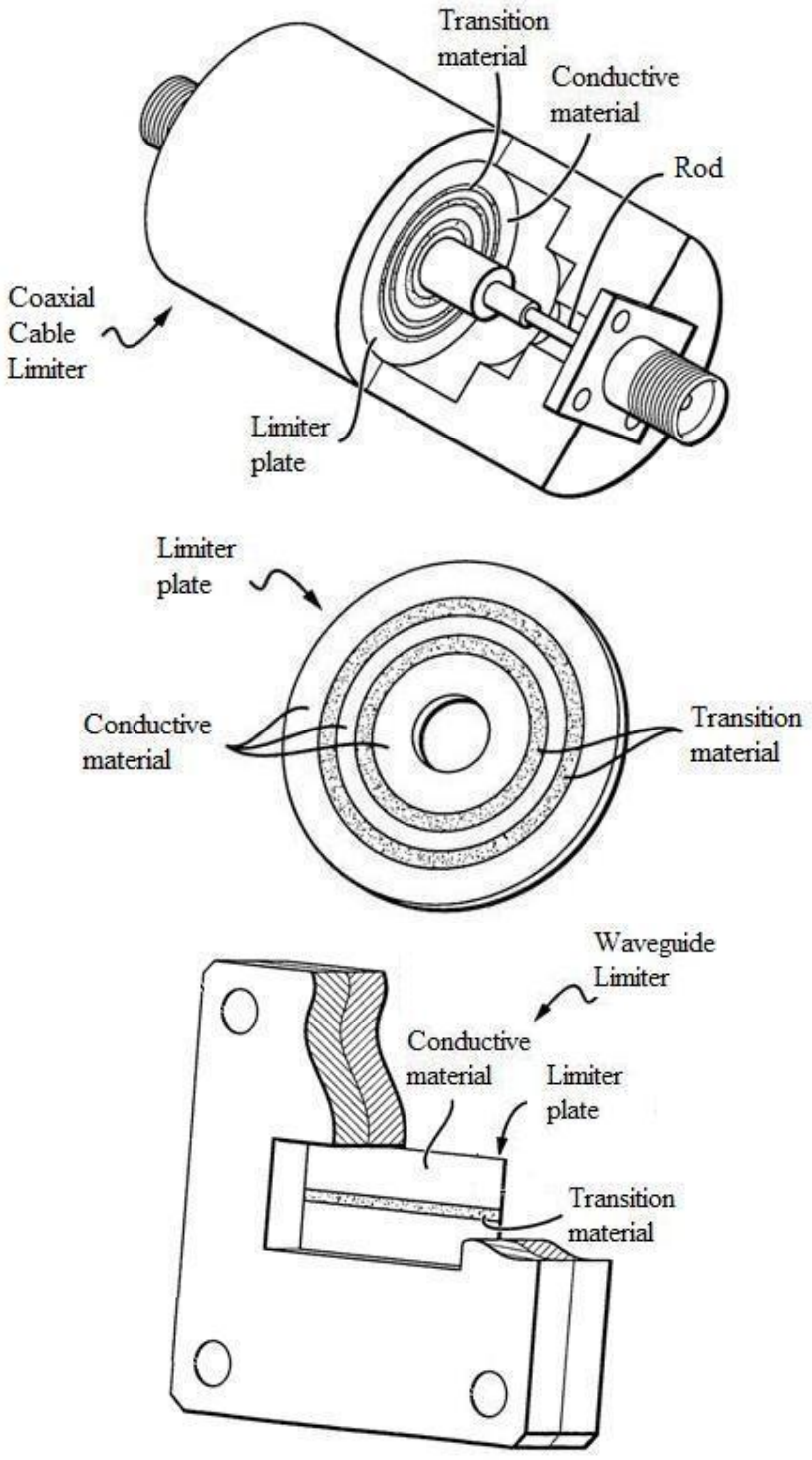

Figure 5-7 : Drawings of coaxial cable and waveguide limiter [3]

This attenuation determines insertion loss of the device. Again, adjustment of the strip width provides flexibility about the threshold level and the maximum power handling of limiter.

In this thesis, one of these two possible structures described above will be realized, tested and discussed to complete this study. Firstly, the most appropriate one should be chosen for the purpose. After a simple overview, the hardest process in the design looks like implementation of the limiter. To make this implementation process easier, the waveguide limiter is selected since the structure of coaxial limiter is more detailed and complex.

After the waveguide limiter is decided, it is time to determine some significant parameters. In this limiter, the width of the aperture is so critical since it may determine the insertion loss and threshold level of the device. Thus, a simulation is run to observe the effects of this parameter on the insertion and return losses before the decision of the aperture's width.

5.2.2. Effect of Width of Capacitive Iris in a Waveguide

In order to decide the width of aperture in the design, a 3-dimensional simulation program, HFSS, is benefited. In this program, the waveguide model is created with some different widths of gap in the middle of the plate as shown in Figure 5-8. Then, the insertion and return losses are simulated for this each width. The results of three possible widths are given in Figure 5-9 and Figure 5-10.

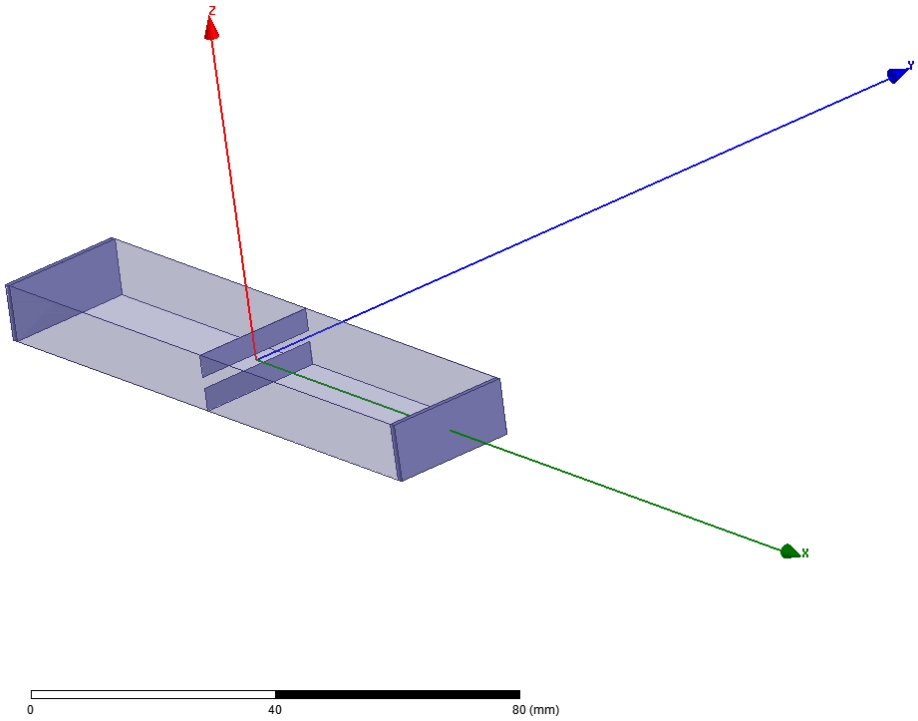

Figure 5-8 : Waveguide model created in HFSS

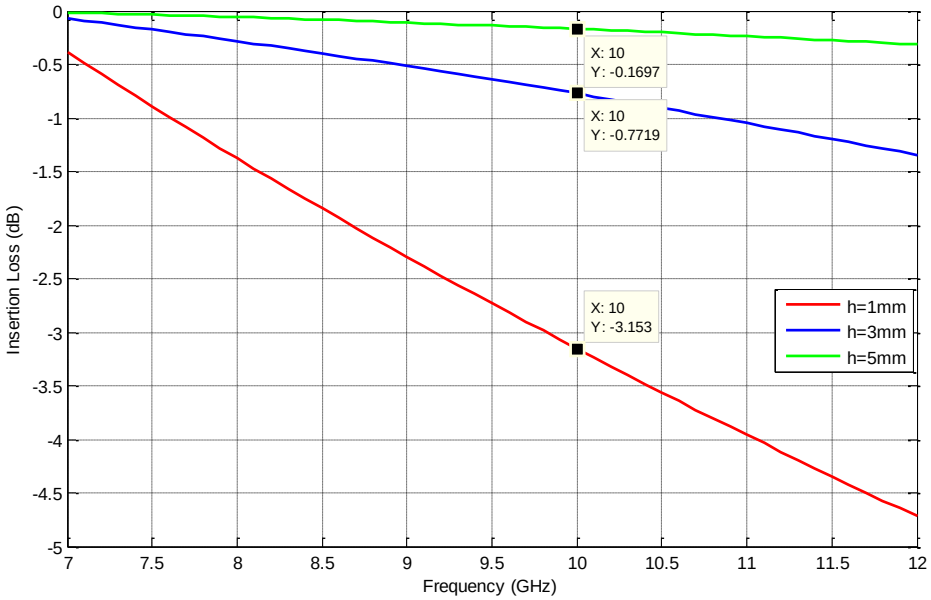

Figure 5-9 : Insertion loss of three different width of capacitive iris

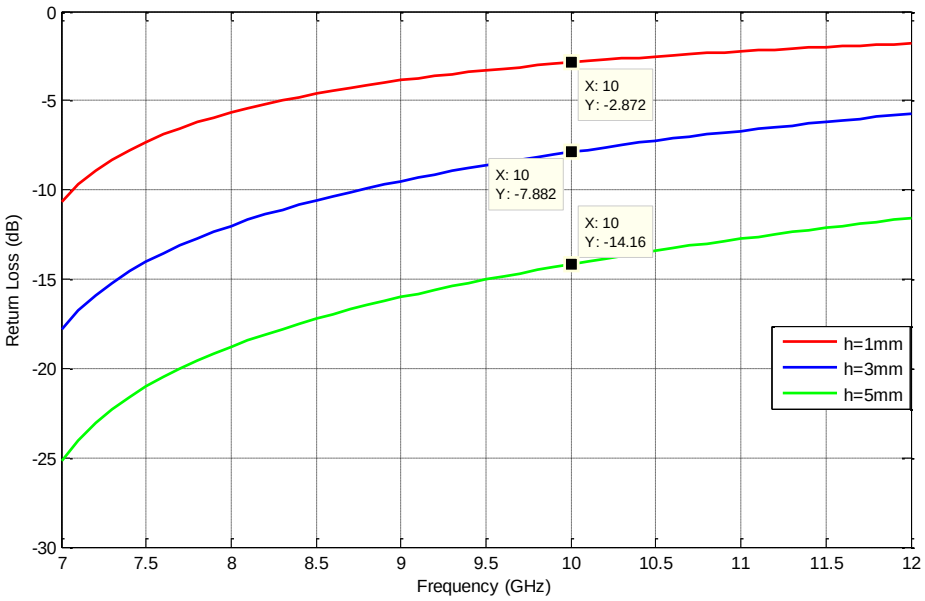

Figure 5-10 : Return loss of three different width of capacitive iris

As expected, when the width of capacitive iris increases, insertion loss of the structure decreases. Since vanadium dioxide used in this gap may cause also some extra losses, the insertion loss should be small. Additionally, if the width of capacitive iris is too large, it is hard to provide the energy which is necessary to heat vanadium dioxide up to transition temperature by sending pulse signal waveforms. On the other hand, it is better to make the gap wider for simpler implementation. When all these reasons are taken into consideration, the widths of capacitive iris are determined as 5 mm for easy implementation and 3 mm for decrease in losses and needed energy to activate the limiter. From the simulation results mentioned above, it is seen that the insertion losses corresponding to these selected widths are about 0.17 dB and 0.77 dB, respectively.

5.2.3. Dimensions of Limiter

After this critical size for limiter design is determined, it is time to work on the horizontal and vertical lengths of the limiter's plate. These lengths mainly depend on the used waveguide in the system. In this thesis, it is generally focused on the

signals at 10 GHz so the selected waveguide should operate at this frequency properly. For this reason, WR90 waveguide is decided to be used in the limiter design. The operating frequency of WR90 is between 8.2 GHz and 12.4 GHz and its length and width are 22.86 mm (0.9 inches) and 10.16 mm (0.4 inches), respectively. According to these dimensions, the sizes of the waveguide limiter are determined by also taking into account safety margins for proper assembly of waveguide and VO_2 limiter. These safety margins are decided as approximately 2 mm from each side. Therefore, the limiter should be a rectangle whose outer dimensions are 27 mm and 14 mm and also, it has an inner rectangle that has 22.86 mm length and 3 mm or 5 mm width as shown in Figure 5-11. As described in the beginning of this chapter, the outer part of the plate has to be a conductor whereas the inner rectangle is expected to be a transition material, VO_2 in this case. In addition to these, another significant parameter could be the thickness of the plate since this quantity affects the distance between two WR90 waveguide pieces after assembly. Thus, if the distance is too large, these two pieces may not be perfectly matched to each other. This might also affect the return loss of the limiter slightly. Therefore, this dimension will be also examined in this chapter.

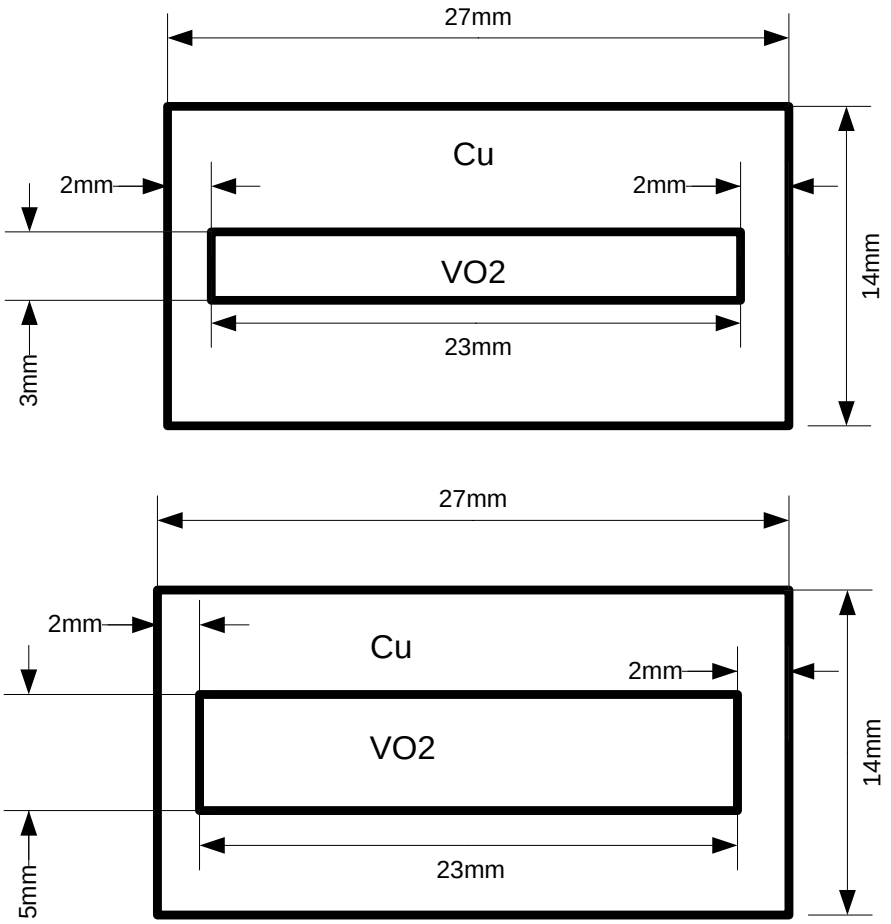

Figure 5-11 : Drawings of limiter plates of waveguide limiter

5.2.4. Manufacture of Designed Limiters

First of all, a conductor plate is cut and shaped out as shown in Figure 5-12 by a lathe machine. For this purpose, a 1 mm brass metal sheet is selected as a conductor and a 5 mm aperture is extracted from this sheet in the design. After shaping the conductor sheet, it looks like Figure 5-12.

Figure 5-12 : Conductor plate shaped by a lathe machine and first prototype of limiter plate

Then, one side of this plate is covered by a piece of tape and VO_2 particles are poured inside this punched plate until the strip in the middle of the plate is totally filled up with VO_2 powders. In order to confine these VO_2 particles to this strip, a piece of tape is again taken to cover the other of the plate. At this point, the first prototype of the limiter design is completed and it is shown in Figure 5-12.

After that, two waveguide to SMA adapters are used to measure the responses of the designed device. For this purpose, this limiter is fixed to one of these adapters by the help of the tape and then this structure is connected to the second waveguide to SMA adapter by placing four screws at the edges of the adapters as illustrated in Figure 5-13.

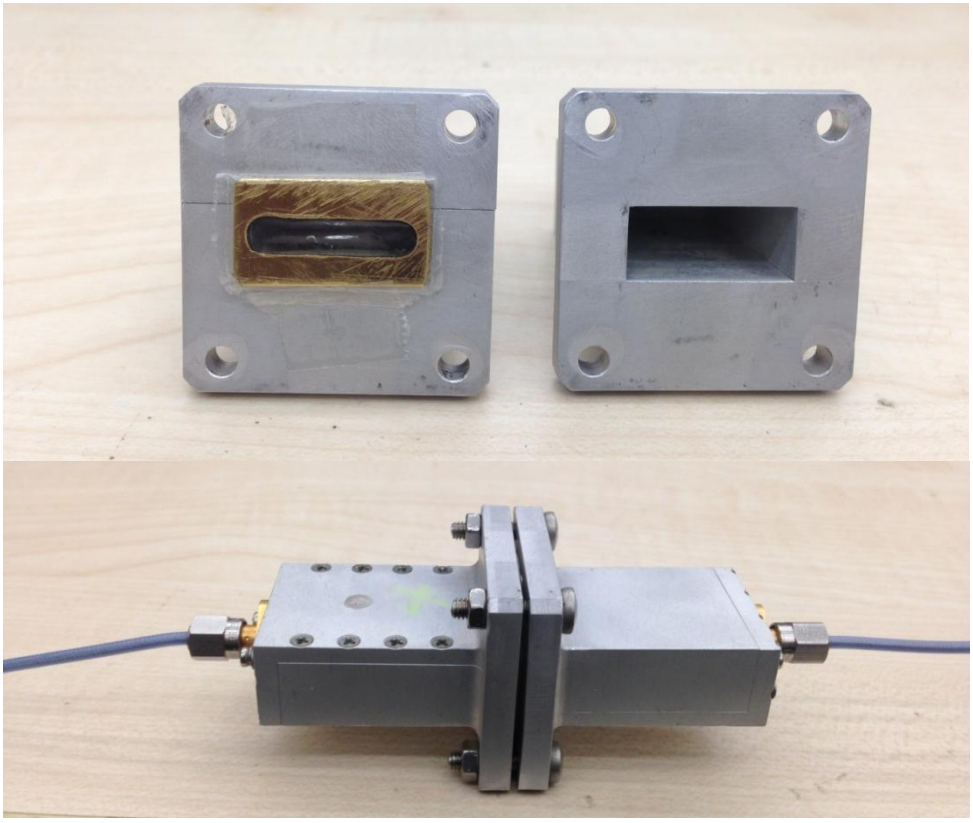

Figure 5-13 : Two SMA-waveguide adapters and limiter plate before and after assembly

This prototype is connected to a Network Analyzer to measure the insertion and return losses of the design after calibration of the Network Analyzer is done. The result of this measurement is given in Figure 5-14. It is seen that the insertion loss of this limiter is 4.86 dB at operating frequency, 10 GHz in this measurement. This value is too high for a limiter used at the front-end of a radar receiver. In order to improve the loss performances of the device, the thickness of the conductor plate and the width of capacitive iris on this plate are altered one by one. The effects of these variations are observed to choose the most suitable combination for the VO_2 limiter.

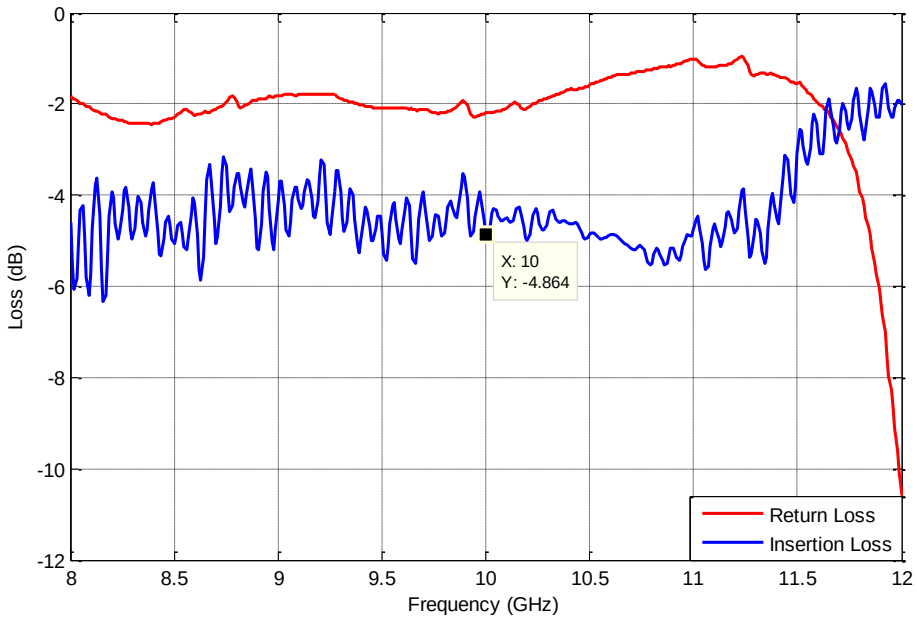

Figure 5-14 : Insertion and return losses of 1 mm brass plate with aperture of 5 mm

First of all, the thickness of limiter is decreased to 300 micrometer without any change at the width of capacitive iris by shaping a 300 um copper sheet. The measurement is repeated under the same conditions with this new design given in Figure 5-15. Figure 5-16 shows the insertion and return losses of this limiter. When the value at only operating frequency is considered in the figure, insertion loss is managed to decrease to 2 dB. There are two main reasons of this improvement. The first reason is the decrease in the amount of VO_2 particles in the strip since as RF signal passes through less VO_2 particles, this results in a relatively low loss in the signal. Another important reason is the better match of the adapters holding the conductor plate. In other words, the adapters can compress and cover the conductor plate more effectively by thinning this plate down.

Figure 5-15 : General view of 300 um copper plate with aperture of 5 mm

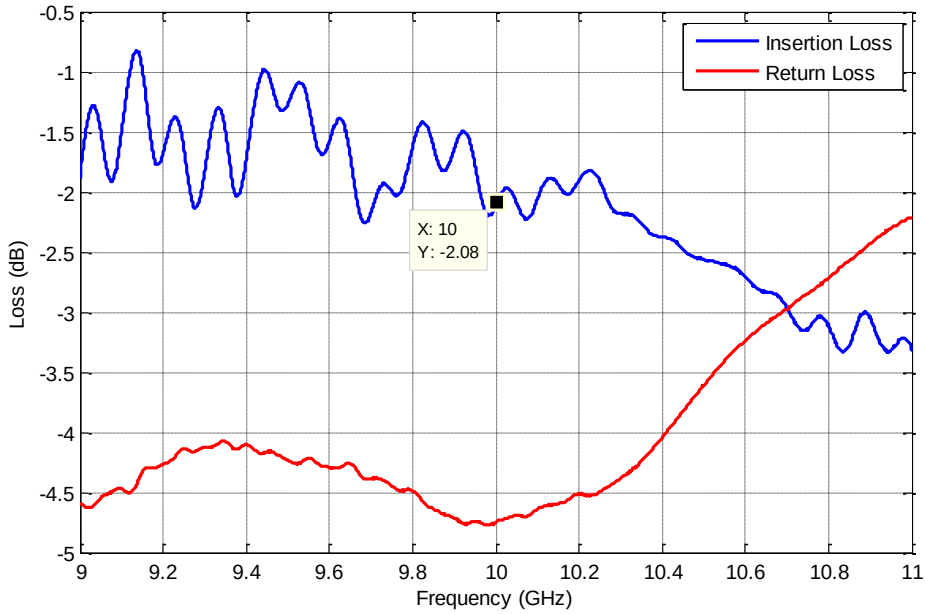

Figure 5-16 : Insertion and return losses of 300 um copper plate with aperture of 5 mm

Next, the width of the capacitor iris is adjusted to 3 mm while the conductor plate's thickness is fixed at 300 um. The insertion and return losses of the device at this state are given in Figure 5-17 and the insertion loss of the limiter at 10 GHz is 2.19 dB as seen in this figure. This is an expected result because as mentioned before, when the width of capacitive iris decreases, insertion loss of the structure increases.

When these three designs are evaluated, the limiters whose thicknesses are 300 um have significantly small losses compared to thicker one. Therefore, it is obvious that 300 um copper sheet is the more appropriate for the VO_2 limiter design. Thereafter, the 300 um copper sheet is decided to be used as the conductor plate of the limiter.

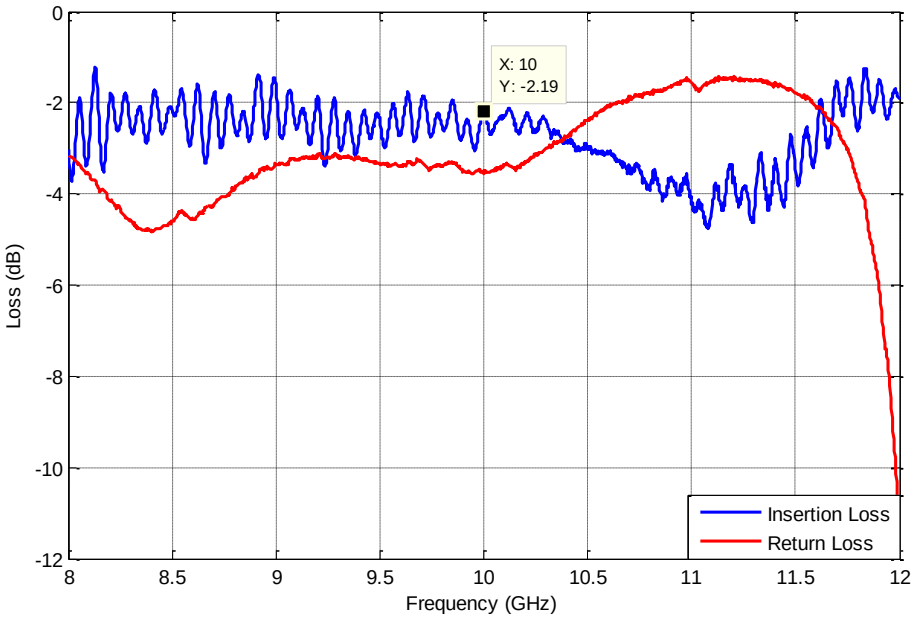

Figure 5-17 : Insertion and return losses of 300 um copper plate with aperture of 3 mm

5.2.5. Effect of Measured Resistance Change on Limiter Performance

In order to understand the effects of measured resistance change in 5.1.2.1., the variation in resistance obtained from characterization stage is simulated with a modeled limiter in HFSS as illustrated in Figure 5-18. The insertion and return losses of the device are observed with different resistance values. Firstly, the copper plate with 3 mm aperture is created and this plate is placed into a WR90 waveguide in this simulation. Then, inside the aperture is filled with a dummy material. By changing the conductivity of this material, the insertion loss is

adjusted to 4.8 dB. For this insertion loss value, the conductivity of the material used to simulate the real VO_2 sample should be adjusted to 0.7 S/m in this program.

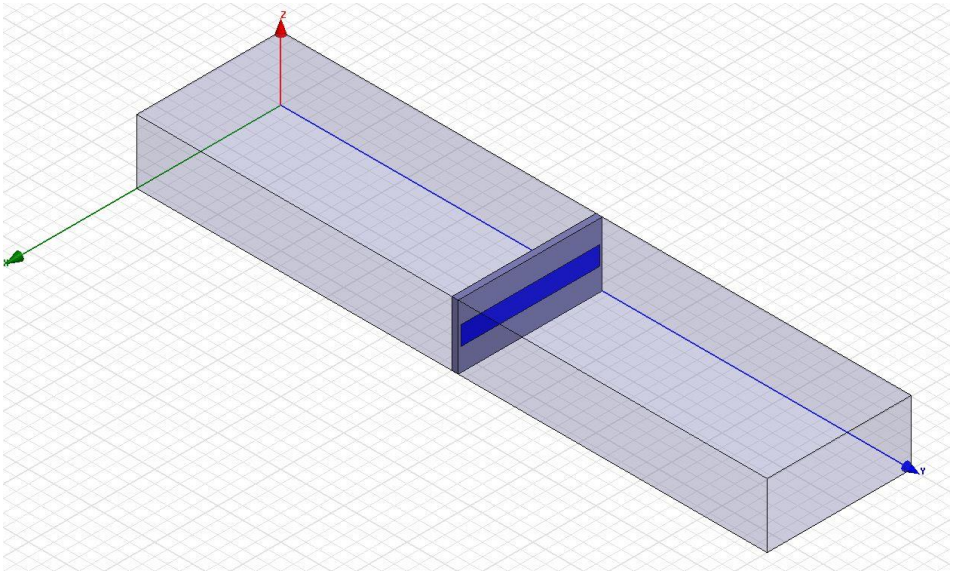

Figure 5-18 : Modeled limiter in HFSS

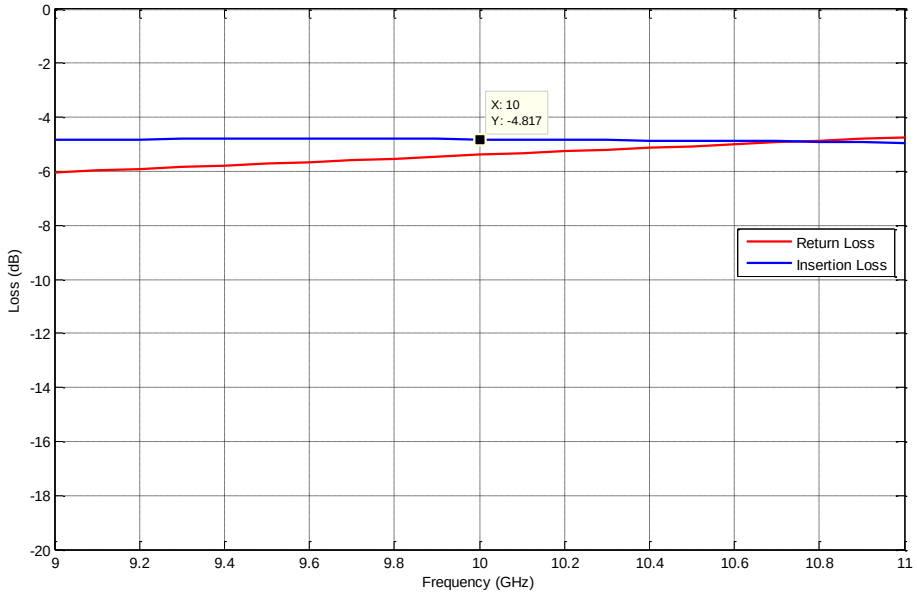

Figure 5-19: Insertion and return losses of modeled limiter with conductivity of 0.7 S/m

After that the conductivity of the material is increased in the same amount of the resistance variation at VO_2 samples. Since the worst scenario is taken into account in this simulation, it is assumed that the resistance decreases by only 10 times. Thus, the conductivity increases by 10 times and it is set to 7 S/m. When this program is run with this conductivity value, the insertion loss of the device is measured as 16.7 dB as shown in Figure 5-20. To sum up, this measured resistance change results in an extra insertion loss of 11 dB which shows that this structure is expected to work as a limiter if temperature of the device is properly increased up to transition temperature.

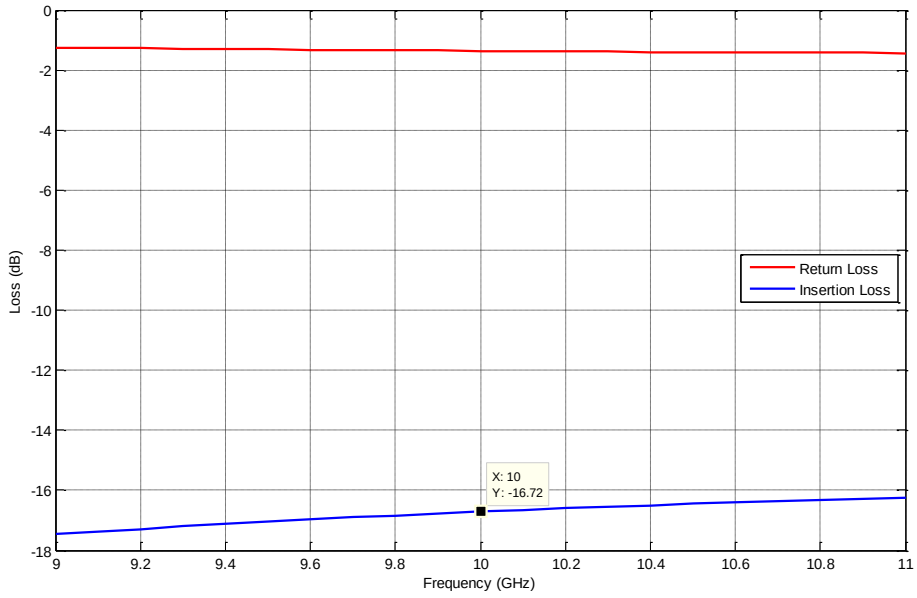

Figure 5-20 : Insertion and return losses of modeled limiter with conductivity of 7 S/m

5.2.6. Measurement Setups

During the design process of VO_2 limiter, a measurement setup is needed to observe the insertion loss of the limiter. For this aim, two different circuit configurations are established with the same circuit components. The purpose of these configurations is to expose two pulses with different amplitudes to the

designed limiter and to observe the differences. While the first pulse cannot activate the limiter, the energy of the second pulse is high enough to heat VO_2 in the limiter up to transition temperature, 67°C. When the outputs of these two circuit configurations are compared, the behaviors of the limiter against two different amplitude pulses are successfully determined since the total losses of the circuit strips are the same for these two configurations except the designed limiter.

The necessary circuit components for both measurement setups are RF power amplifier, circulator, 20 dB high power attenuator, 20 dB low power attenuator and the designed limiter. In the first configuration as shown in Figure 5-21, the RF amplifier is firstly placed to supply the high power RF pulse to the circuit and right after; a circulator is needed to prevent the RF amplifier from return of the sending RF pulse. Next, before the limiter, attenuators are used to weaken the produced high power RF pulse and to send pulse with low amplitude to the limiter. This configuration is called as test setup 1. In the second configuration, the only difference is the places of attenuators and limiter. In other words, the limiter is connected to the circulator instead of attenuators as shown in Figure 5-22. By establishing this configuration, the limiter is exposed to high power microwave pulses. Then, the limiter is activated by the help of this high energy and attenuates the coming RF pulse as mentioned before. This second configuration is called as test setup 2.

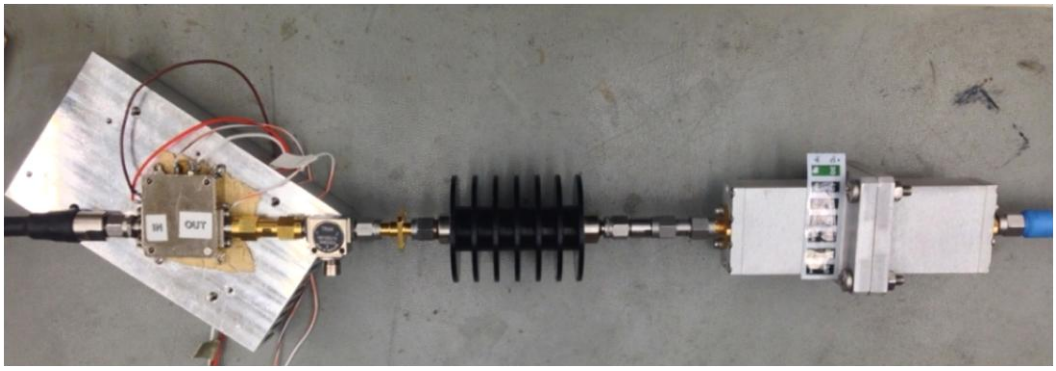

Figure 5-21 : Test Setup 1 that sends low-amplitude pulses to the limiter

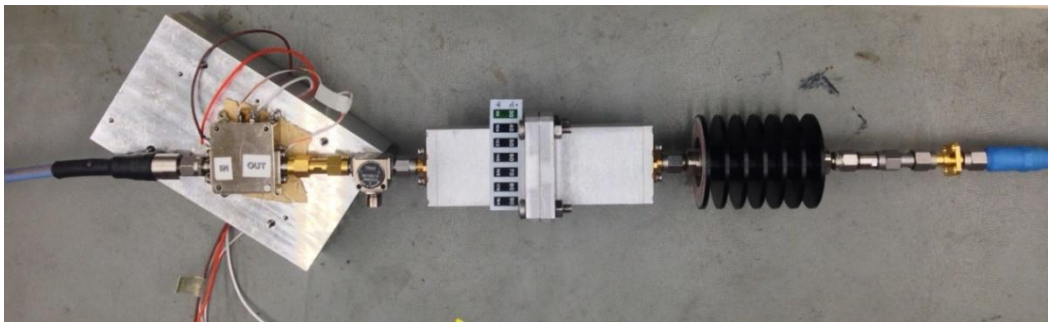

Figure 5-22 : Test Setup 2 that sends high-amplitude pulses to the limiter

The RF amplifier needs some DC voltages, namely, +5V, -5V, +9V and a TTL switching signal as explained in Chapter 3. After these are applied to the amplifier properly, a signal generator is connected to this circuit to get a 19 dBm continuous wave at 10 GHz. And then, the amplifier is ready to send the HPM pulses.

It is time to measure the output of circuits by using a spectrum analyzer. Firstly, the signal generator and spectrum analyzer are locked to each other by using external 10MHz signal of signal generator in order to increase the accuracy of the frequency measurement. Then, settings of the spectrum analyzer are arranged to measure a pulse RF signal at 10 GHz. These settings are center frequency (10 GHz), span (zero span), sweep time (30 us), level and scale of amplitude. Next, two circuit configurations are measured separately and pulse shapes are compared to each other to observe any effect caused by DUT (Device Under Test).

5.2.7. Measurements of Designed Limiters with VO_2 in powder form

In the first trial, the limiter that has 300 um thickness and 5 mm aperture filled up with VO_2 particles is placed between two SMA to waveguide adapters. The insertion loss of this limiter is measured with test setup 1 and 2 at several times, but there is no difference between these two measurements in terms of insertion loss of DUT. Then, the adapters are dismounted to try the second VO_2 samples. When the screws of waveguide are removed, it is seen that the tape on the VO_2 particles is burned and damaged as shown in Figure 5-23. As shown from this figure, the tape

is warmed up from the middle of the structure as expected because the electric field strength is larger at the middle of the waveguide structure.

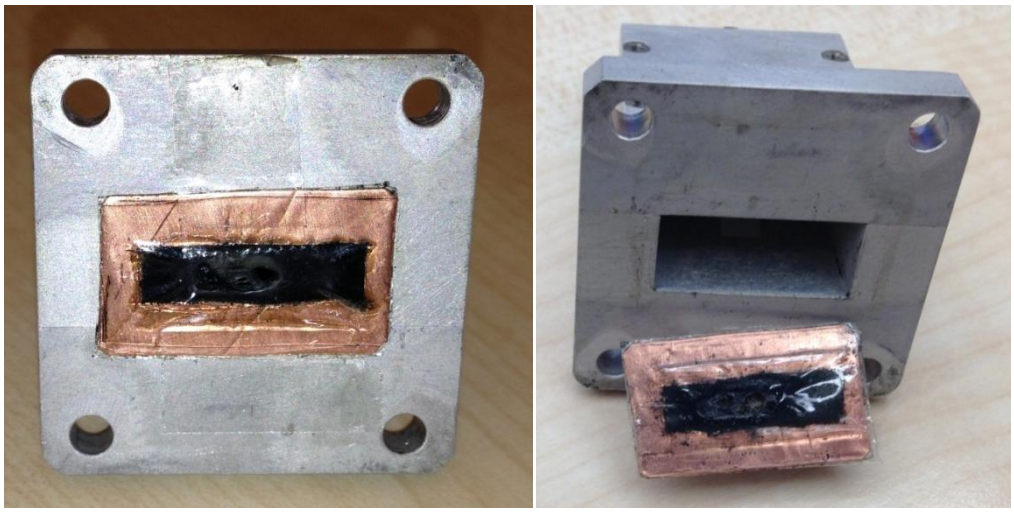

Figure 5-23 : General views of damaged limiter plate

In this event, the tape is firstly suspected to absorb the coming RF signal and to be damaged due to the signal energy. Therefore, the test is repeated only using a piece of tape and copper plate without any VO_2 particles. After sending RF pulse again, it is seen that there is no damage on the DUT. Thus, it is decided that the absorption of RF signal is caused by VO_2 and this absorption of the energy leads to heating of the limiter structure. Finally, this high heat can burn the tape on the VO_2 particles. In order to continue these trials, the tape problem is handled by using another type of tape that can resist to heat.

In the second trial, the same copper plate and VO_2 particles are assembled with this new tape in the same manner and Figure 5-24 shows the designed limiter.

Figure 5-24 : Limiter plate assembled with new tape

Then, it is time to measure the limiter with new tape. Although the insertion loss of this limiter is measured with test setup 1 and 2 at several times, there is no difference in terms of insertion loss of DUT again.

Next, the limiter is formed by using the other VO_2 sample and measured with the same test setups. After that, two VO_2 samples are separately assembled with 300 um copper plate having 3 mm aperture and measured in the same way again. In all these configurations, it is observed that there is no difference in terms of insertion loss of the limiters. In other words, the designed devices do not work as a limiter.

When this unexpected result is evaluated, it is thought that there are unavoidable air gaps between the VO_2 particles since VO_2 samples are in crystalline and powder forms. These air gaps cause discontinuities in electrical conductivity of VO_2 aperture. Thus, even if the resistivity of VO_2 particles decreases during the state change of the material, this resistivity change cannot affect the insertion loss of the device due to these discontinuities in VO_2 particles.

5.2.8. Measurements of Designed Limiters with VO_2 in a more solid form

In order to overcome the discontinuity problem of VO_2 particles, VO_2 samples in a more appropriate form should be obtained. Therefore, some different forms are tried to find that increase the conductivity of the aperture filled up with VO_2 particles.

First of all, VO_2 particles are combined with some water in a beaker and they are stirred up until the VO_2 particles are totally dissolved in water. Then, this liquid solution is directly poured to the aperture in the copper plate and this plate is confined by a piece of tape again. After that, the insertion loss of the designed limiter is measured with test setup 1 and 2. When these obtained losses are compared to each other, it is seen that they are nearly the same again.

Secondly, VO_2 particles are combined with some water and they are stirred up until the VO_2 particles are totally dissolved in water again. Next, the 5 mm aperture is filled up with this prepared liquid solution and the solution is left to dry in the copper plate. A half-day later, the solution is completely dried and takes shape of the aperture and then, the copper plate is covered by a piece of tape to prevent the dispersion of VO_2 in the aperture. Again, test setup 1 and 2 are constructed to measure the difference in the insertion loss between these two conditions. Eventually, the designed limiter can give different responses to high and low amplitude signals as desired. For this purpose, the period of the RF pulse is fixed to 10 us and the duty cycle of the signal is swept from 20% to 80% in order to measure and observe the insertion losses corresponding to different pulses. The outputs of the test setup 1 and 2 for different pulse widths are given in Figure 5-25, Figure 5-26, Figure 5-27 and Figure 5-28, successively. The effect of the limiter is the difference between successive graphs in the given figures. Also, these results are also tabulated in Table 5-2 to present the results in a better way.

Table 5-2 : Results of limiter having 5 mm aperture

Pulse Width of the Signal	**Result of Test Setup 1 (Peak Power)**	**Result of Test Setup 2 (Peak Power)**	**Effect of the Limiter**
2 us	-6.46 dBm	-7.26 dBm	0.8 dB
3 us	-6.57 dBm	-7.80 dBm	1.23 dB
5 us	-6.82 dBm	-8.17 dBm	1.35 dB
8 us	-7.21 dBm	-8.76 dBm	1.55 dB

From Figure 5-25, when the pulse width of signal is adjusted to 2 us, the effect of the limiter is observed as 0.8 dB in amplitude. As Figure 5-28 is focused on, the effect of the device reaches to 1.55 dB.

When the results in Table 5-2 are evaluated, the outputs of the test setup 1 are varied with different pulse widths due to the characteristics of the RF amplifier. In other words, the output power of RF amplifier decreases while the pulse width of the signal increases. Another significant point is that when the pulse width of the signal increases, the attenuation caused by the limiter also raises since the maximum temperature of VO_2 in the aperture during the operation rises.

However, if the pulse width is increased to more than 5 us in this test setup, it is observed that the limiter has attenuation more than 4 dB momentarily but after a while the designed limiter is damaged and the performance of the limiter degrades. Before the signal having 8 us pulse width is applied to the limiter, it can change states between semiconductor to conductor again and again according to its temperature. However, this large pulse width results in irreversible damage on the limiter and the beginning state of the limiter cannot be reached anymore.

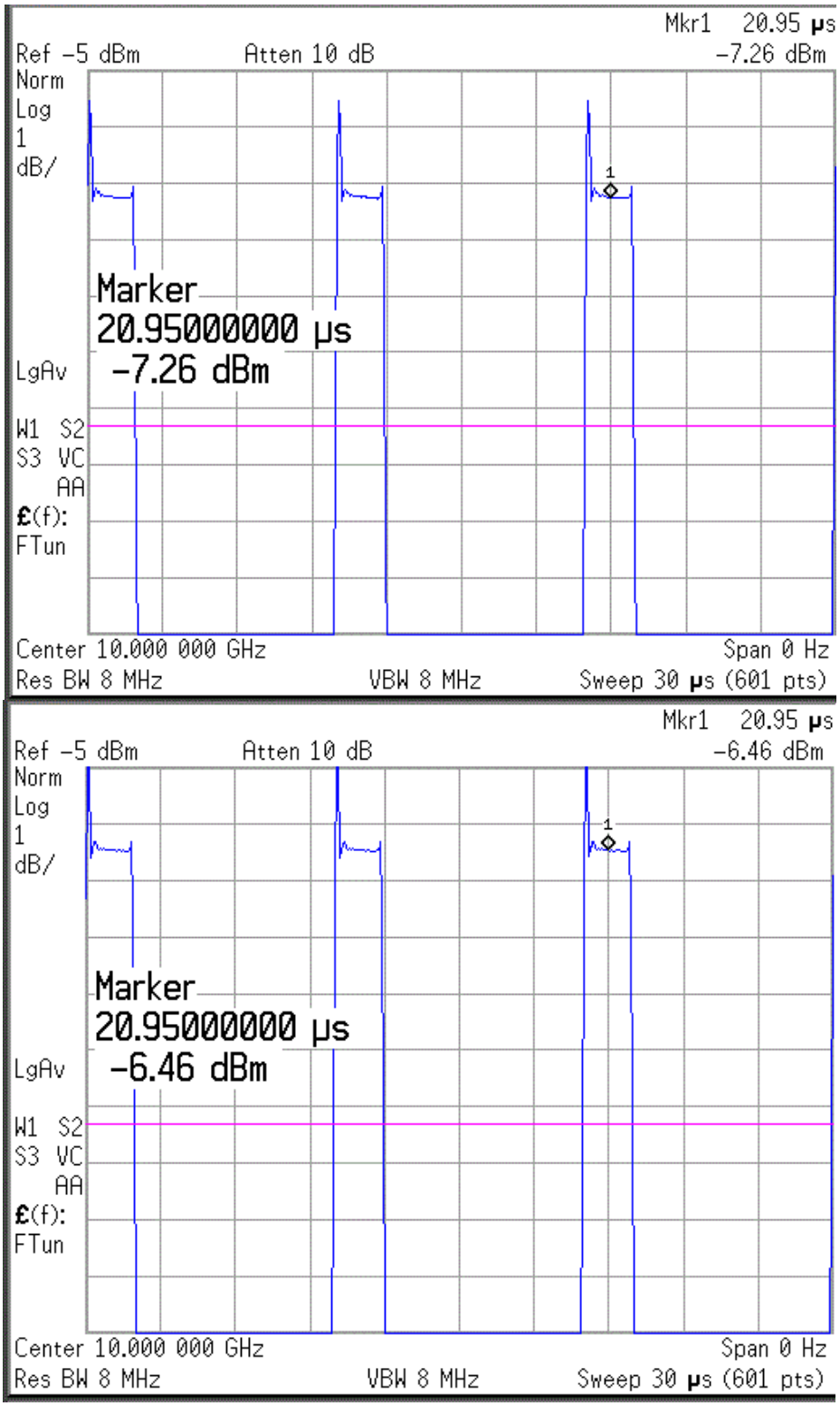

Figure 5-25 : Responses of limiter having 5 mm aperture in test setup 1 and test setup 2 with pulse width of 2 um

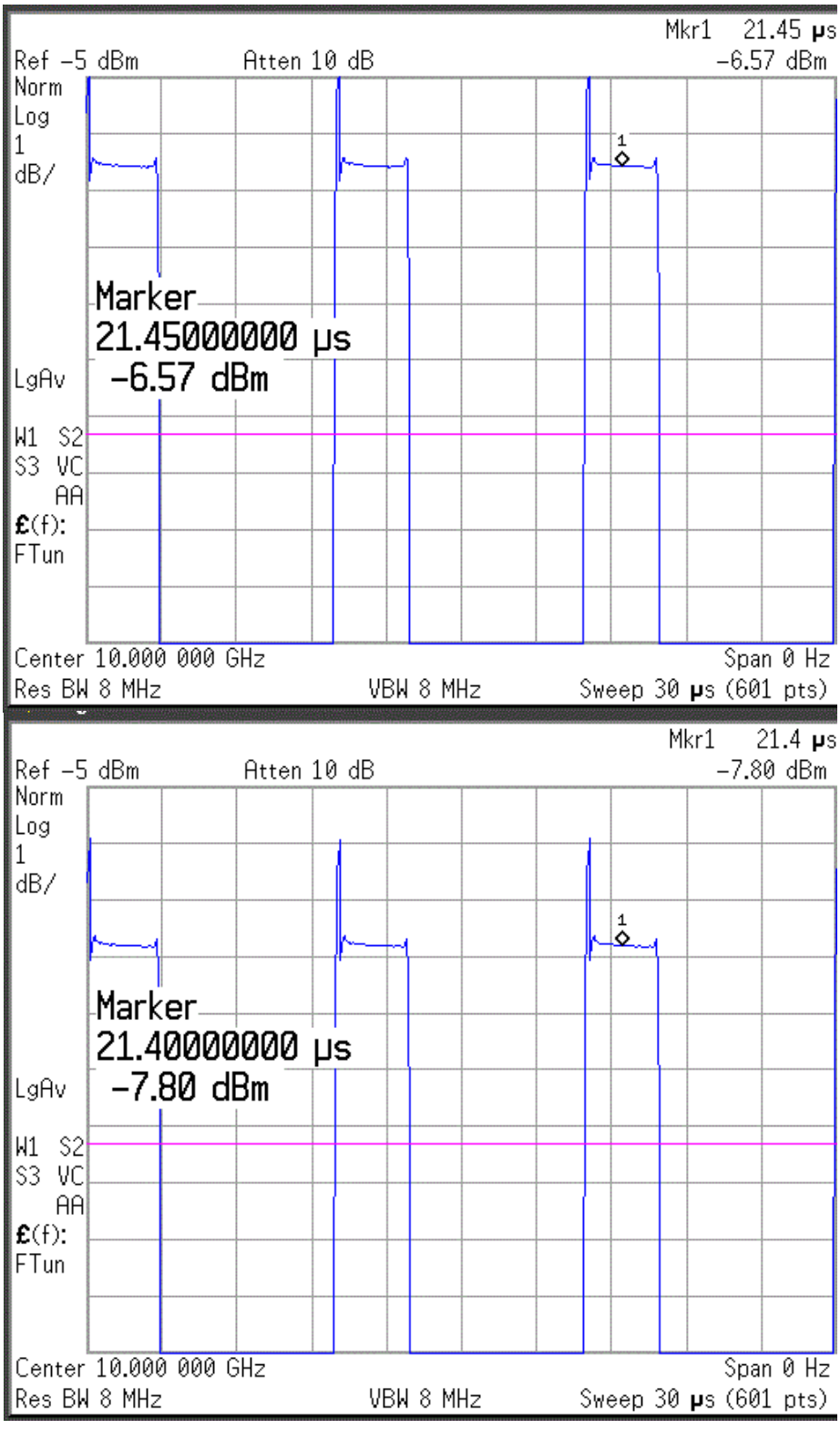

Figure 5-26 : Responses of limiter having 5 mm aperture in test setup 1 and test setup 2 with pulse width of 3 um

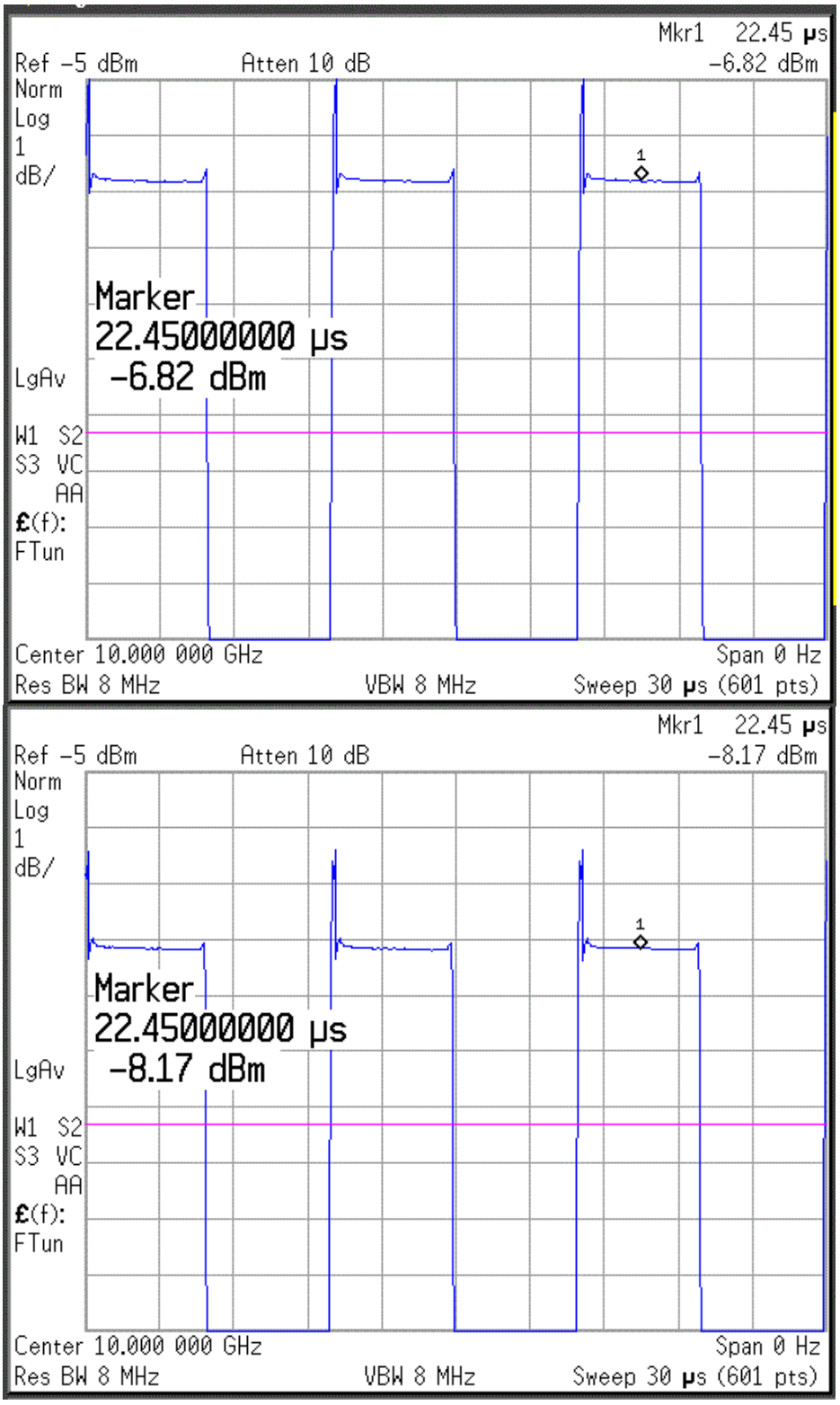

Figure 5-27 : Responses of limiter having 5 mm aperture in test setup 1 and test setup 2 with pulse width of 5 um

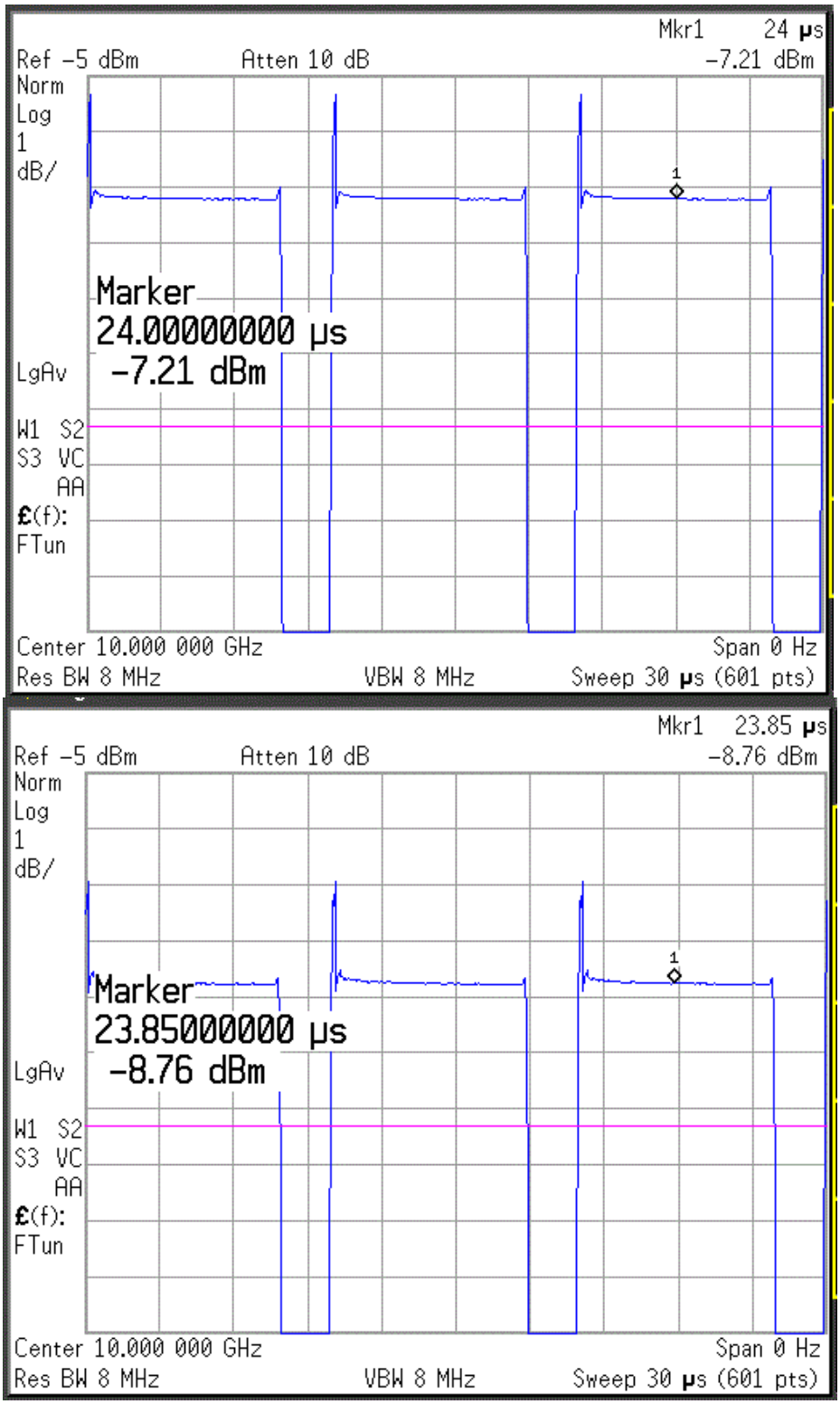

Figure 5-28 : Responses of limiter having 5 mm aperture in test setup 1 and test setup 2 with pulse width of 8 um

In order to improve the performance of the VO_2 limiter, the aperture on the plate is narrowed. Instead of 5 mm aperture, a copper plate having a 3 mm aperture is decided to be used with the same VO_2 sample and a piece of tape while assembling the limiter. The outputs of the test setup 1 and 2 for different pulse widths are given in Figure 5-29, Figure 5-30, Figure 5-31 and Figure 5-32, successively again. In this case, the minimum loss difference caused by the limiter is 1.64 dB whereas the maximum insertion loss difference is 2.23 dB according to Table 5-3.

Table 5-3 : Results of the limiter having 3 mm aperture

Pulse Width of the Signal	**Result of Test Setup 1 (Peak Power)**	**Result of Test Setup 2 (Peak Power)**	**Effect of the Limiter**
2 us	-6.13 dBm	-7.77 dBm	1.64 dB
3 us	-6.24 dBm	-8.09 dBm	1.85 dB
4 us	-6.37 dBm	-8.33 dBm	1.96 dB
5 us	-6.49 dBm	-8.72 dBm	2.23 dB

Thus, the decrease in the width of aperture results in better performance against the same RF signals. In this structure, the narrow aperture contains smaller amount of VO_2 particles and the maximum temperature of the limiter having narrow aperture rises more with the same signal. This higher temperature reached during the experiment leads to more conductivity in the aperture and more attenuation at the RF signal.

The pulse width of the signal is limited to 5 us to protect the designed limiter because in the previous experiment, the limiter having 5 mm aperture is damaged due to this larger pulse width.

Moreover, the second VO_2 sample produced with formic acid is also used in limiter design. The structure works with these VO_2 particles in a similar manner but performance of the first sample is slightly better than performance of the second one.

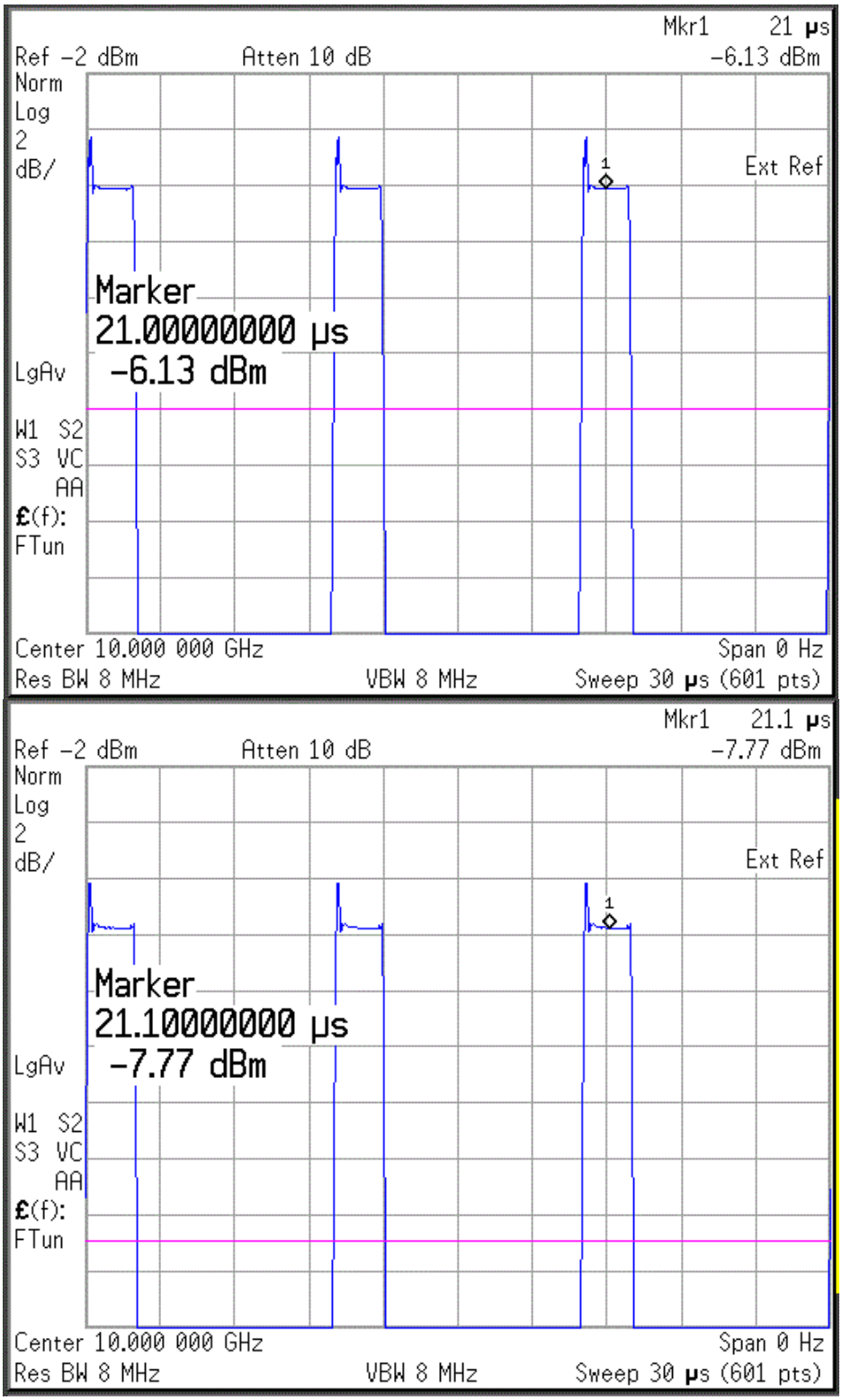

Figure 5-29 : Responses of limiter having 3 mm aperture in test setup 1 and test setup 2 with pulse width of 2 um

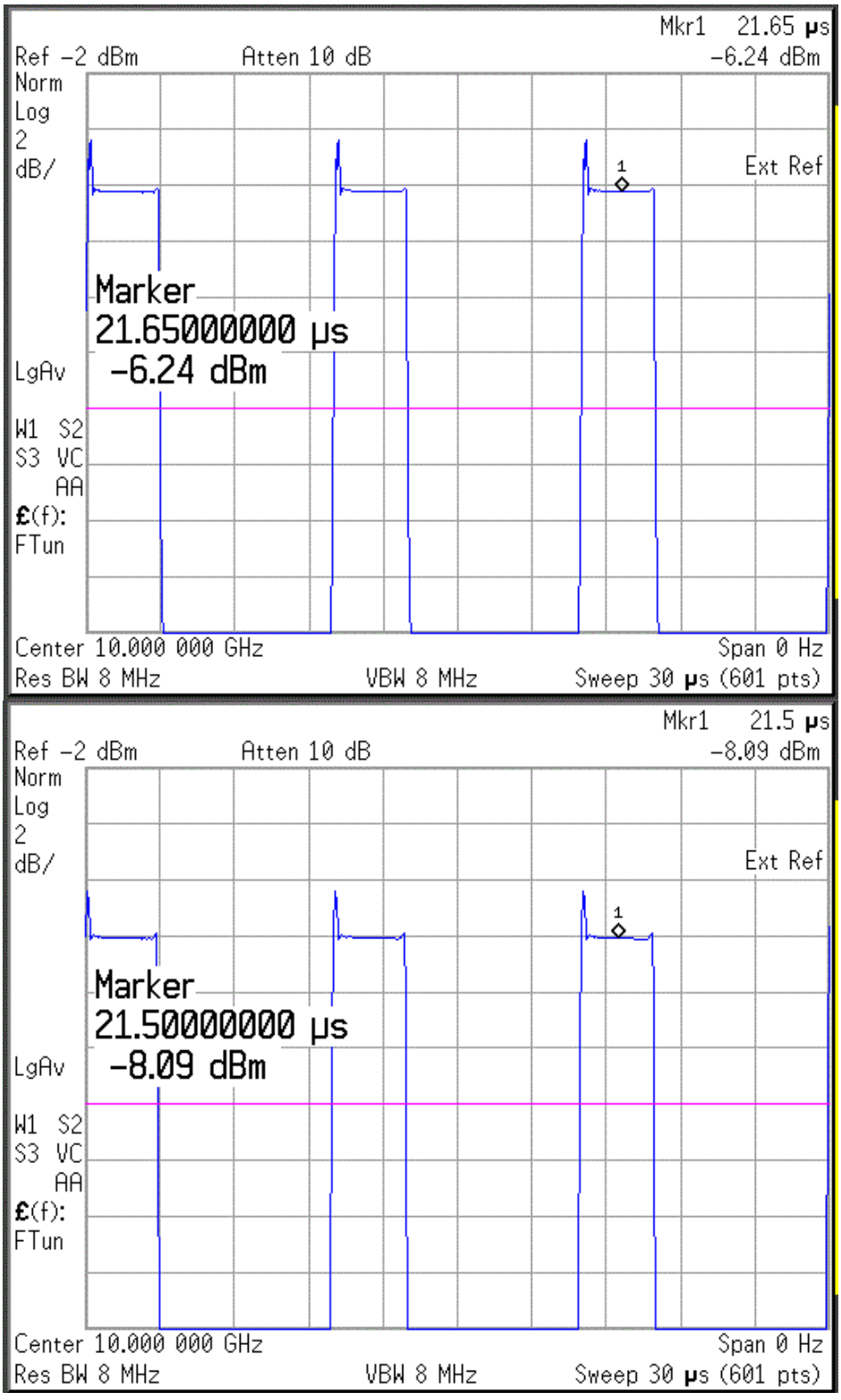

Figure 5-30 : Responses of limiter having 3 mm aperture in test setup 1 and test setup 2 with pulse width of 3 um

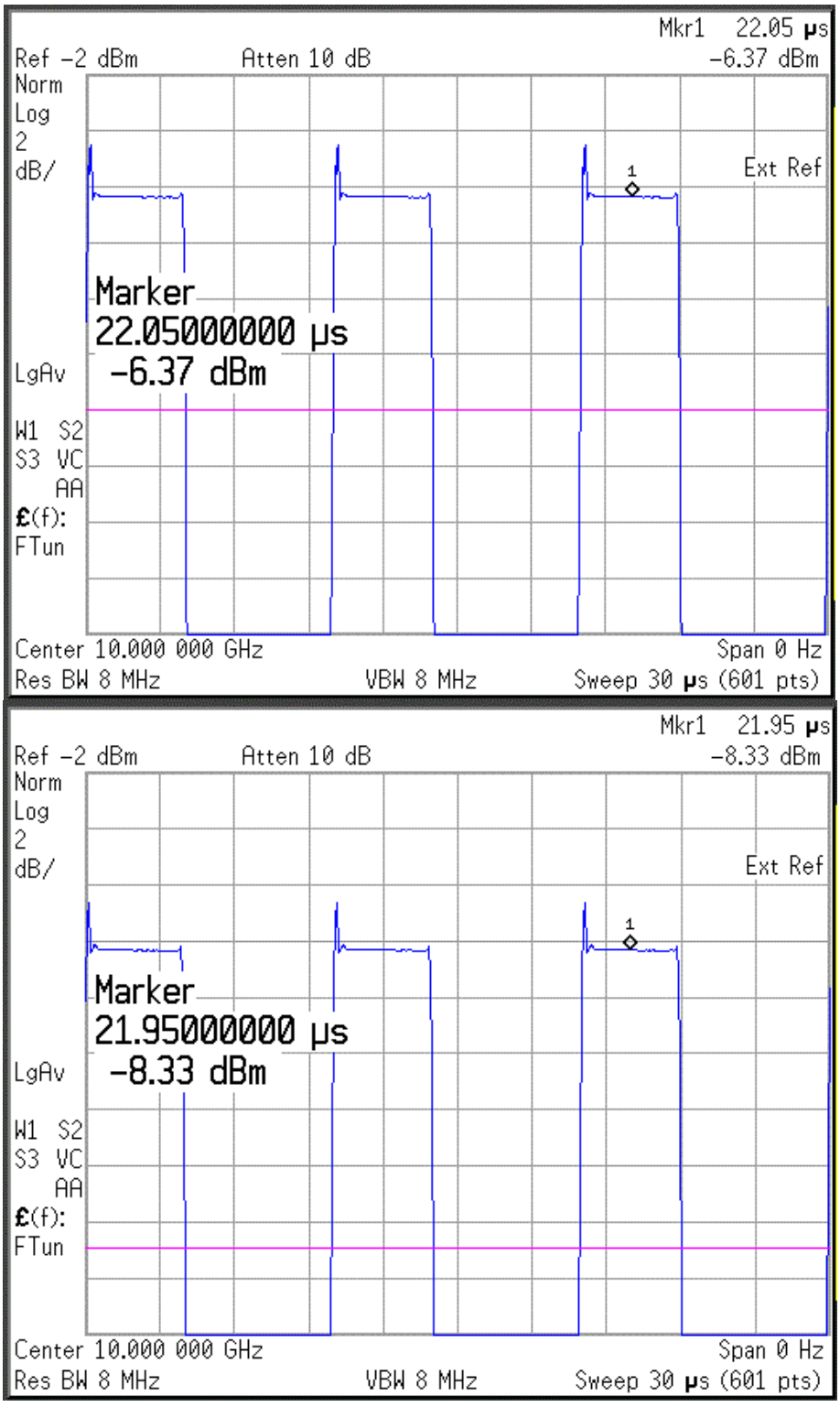

Figure 5-31 : Responses of limiter having 3 mm aperture in test setup 1 and test setup 2 with pulse width of 4 um

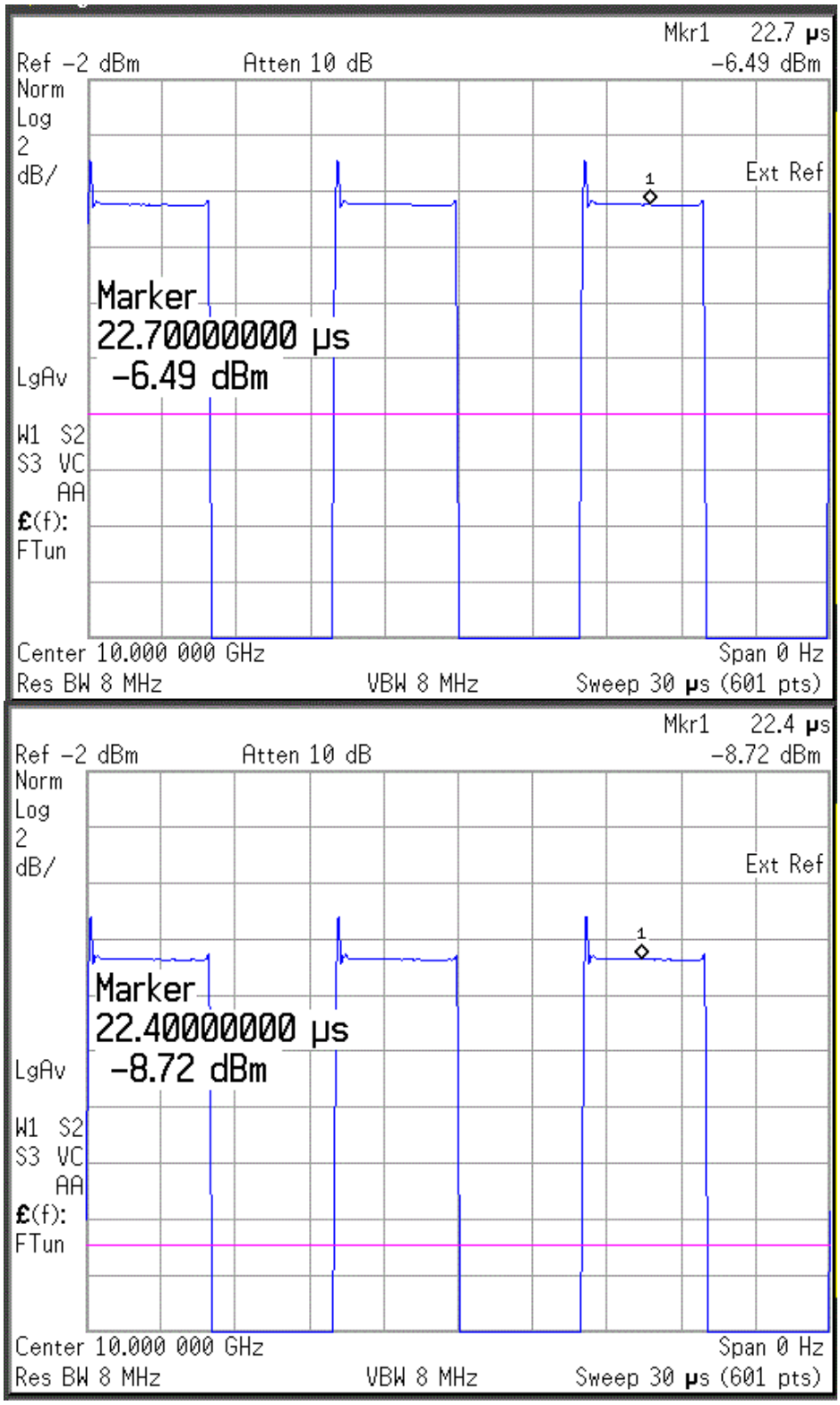

Figure 5-32 : Responses of limiter having 3 mm aperture in test setup 1 and test setup 2 with pulse width of 2 um

5.2.9. Transient Response of Designed Limiter

In this part, the designed limiter is subjected to HPM pulses to observe the transient response characteristics of the limiter. Firstly, HPM pulses are produced and measured by using a high speed oscilloscope. The setup producing the RF pulses is demonstrated in Figure 5-33. It is basically composed of an RF amplifier, a circulator and an attenuator block again. The output of the setup is recorded to have a reference point in this experiment. In the next measurements, any difference from this reference data shows directly the effects of the limiter. The reference waveform is illustrated in Figure 5-34. In this graph, each division corresponds to 20 ns in time axis and 100 mV in amplitude axis. For instance, the peak to peak voltage value of the reference signal is 540 mV at the end of the pulse.

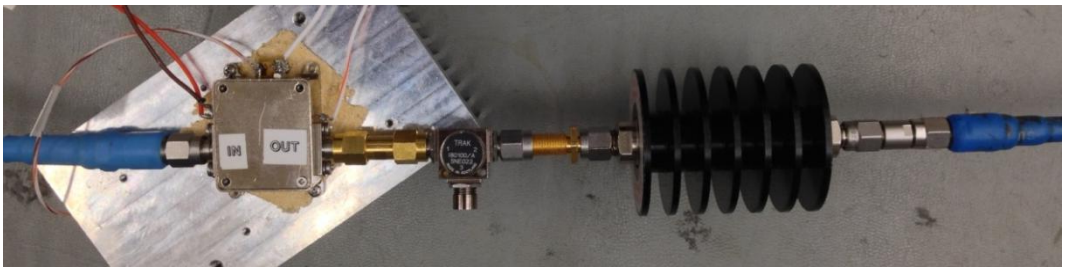

Figure 5-33 : Experimental setup measuring HPM pulses

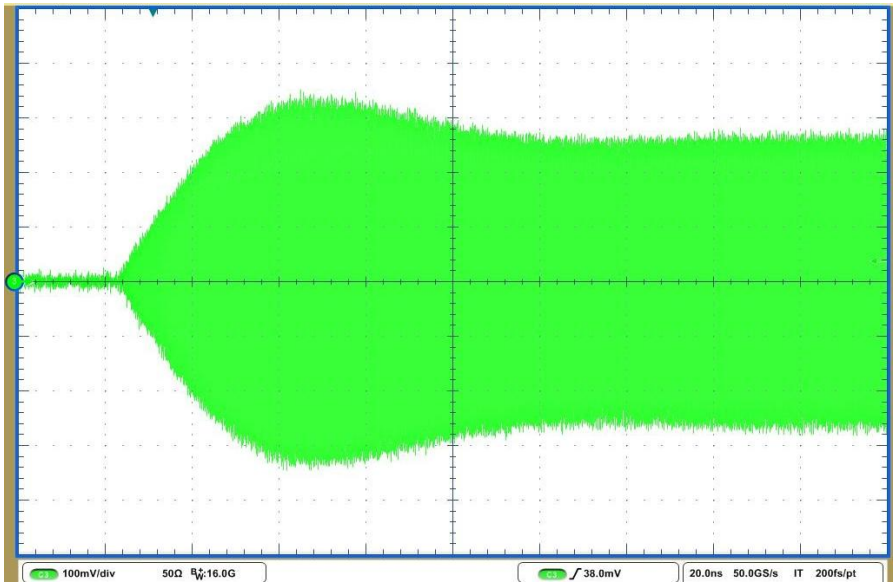

Figure 5-34 : HPM pulse measured in the experimental setup

Then, by only inserting the limiter in the circuit, the usual measurement setup is implemented. The limiter having 3 mm aperture is placed after the circulator and before the attenuator as shown in Figure 5-35.

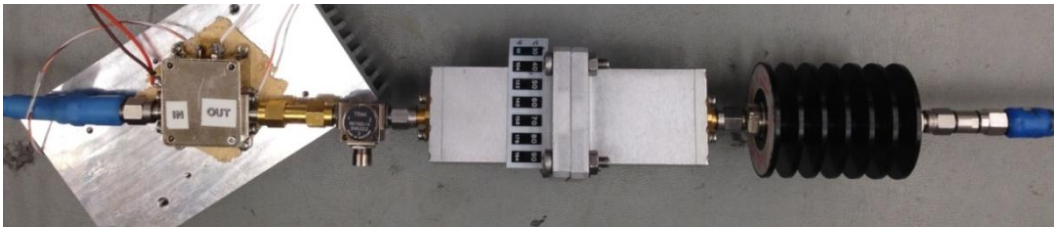

Figure 5-35 : Test Setup 2 that sends high-amplitude pulses to the limiter

In the first measurement, only one HPM pulse is transmitted to the device and the pulse duration of this single pulse is 5 us. Then, the output of the setup is caught by the high speed oscilloscope. This waveform is given in Figure 5-36 and each division corresponds to the same quantities explained above. The peak to peak value is this case is about 300mV at the end of the pulse. In order to observe the response of the limiter to only one RF pulse, the total attenuation is calculated below:

$$Total\ Attenuation(TA) = 20 \times \log(\frac{V_{pp}\ of\ the\ first\ signal}{V_{pp}\ of\ the\ second\ signal})$$

$$TA = 20 \times \log(\frac{540\ \text{mV}}{300\ \text{mV}}) = 5.1\ dB$$

The insertion loss of the limiter before this experiment is measured as 4.76 dB. When these measurement results are compared, the variation at the insertion loss is about 0.34 dB and it can be said that one RF pulse causes a slight loss on the limiter.

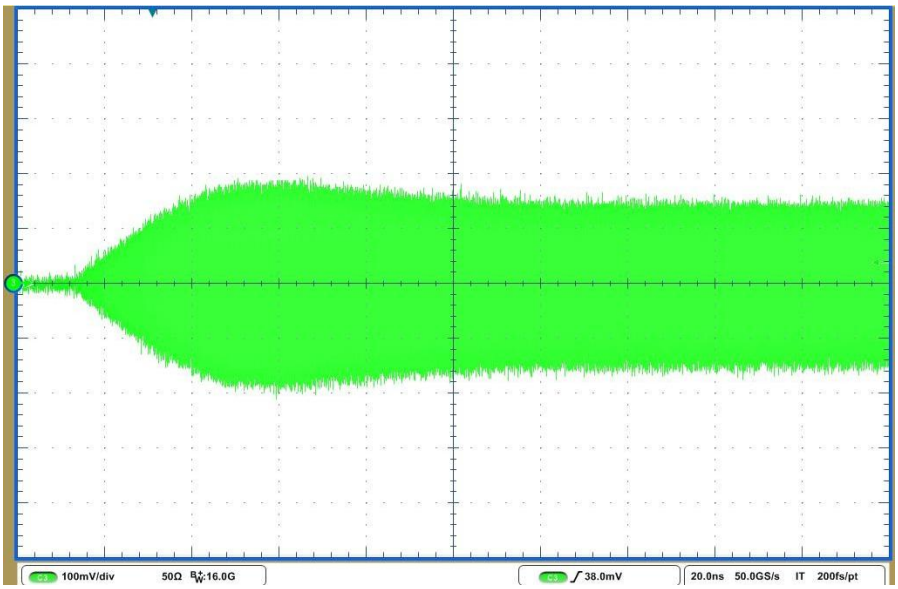

Figure 5-36 : Transient response of designed limiter after only one HPM pulse

Secondly, 10 us period and duty cycle of 50% signal is sent to the limiter by the same measurement setup. After 60 seconds, it is thought that the VO_2 in the aperture heats enough and it is reached a steady state so the output of the device is recorded again as shown in Figure 5-37. The peak to peak value is this case is about 240 mV at the steady state region. In order to observe the limiter response to this pulse train, the total attenuation is calculated below again:

$$Total\ Attenuation(TA) = 20 \times \log(\frac{V_{pp}\ of\ the\ first\ signal}{V_{pp}\ of\ the\ second\ signal})$$

$$TA = 20 \times \log(\frac{540\ \text{mV}}{240\ \text{mV}}) = 7.04\ dB$$

$$Attenuation = TA - IL = 7.04 - 4.76 = 2.28\ \text{dB}$$

The attenuation caused by the limiter is calculated as 2.28 dB when the insertion loss of the limiter measured at room temperature (IL) is extracted from the total attenuation. This 2.28 dB attenuation is consistent with the 2.23 dB attenuation measured with spectrum analyzer in the previous measurements.

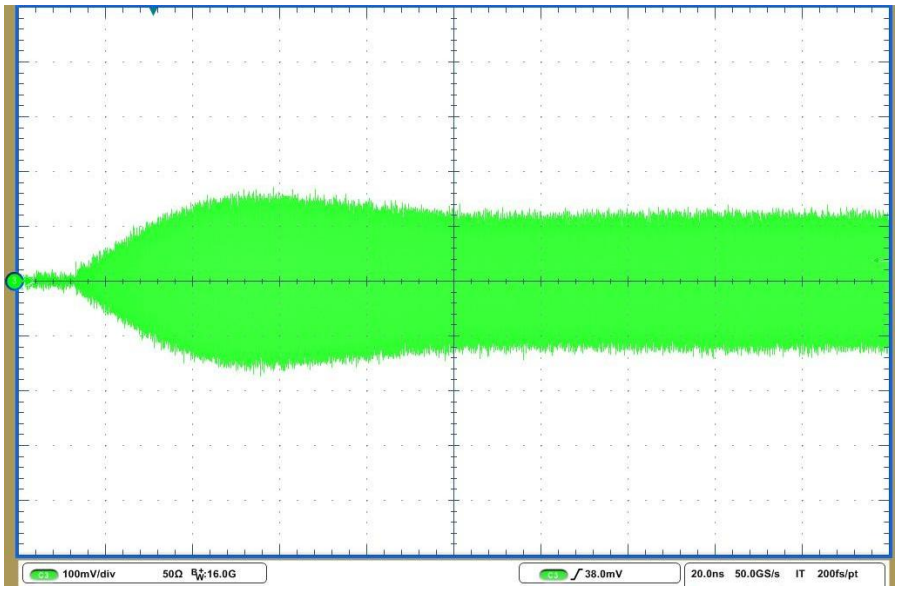

Figure 5-37 : Transient response of designed limiter after 60 seconds

As mentioned in Chapter 3, the effect of the diode limiter, TGL2201, is observed on the signal amplitude after 16.5 dBm amplitude and 10 ns time. In this designed structure, the response time of the VO_2 limiter cannot be certainly determined with these measurements as given in Figure 5-36 and Figure 5-37 but it is certain that only one signal is enough to observe the response of the limiter slightly; that is to say that it is seen the limitation property of the device from even the first pulse. Thus, this VO_2 limiter structure has the ability to response to a sudden threat in a very short time. In addition, as mentioned before, it is claimed that the opening time of the VO_2 limiter is less than 10 ns [3]. After enhancing this design, the response time of this limiter structure can be improved in a significant manner and it is possible to reach a response time in the order of nanoseconds.

CHAPTER 6

CONCLUSION & FUTURE WORK

In this thesis, the VO_2 limiter introduced in a patent [3] is tried to be realized for waveguide structure and some performance parameters are measured in order to propose this device as a method to the HPM pulses. Also, the syntheses and characterizations of VO_2 samples needed for the limiter design are explained in a step by step manner.

Firstly, the specifications of the HPM test facilities and weapons are investigated in chapter 2 to have some idea about today's HPM technology and show the developments of this technology. Then, the resistance variation of VO_2 around the transition temperature is mentioned and the applications using this different property are briefly introduced.

In Chapter 3, the technology of LNA that is the most vulnerable circuit component in a typical receiver system to HPM pulses is firstly studied to prove that 100 ns pulse can damage this device. Next, the destruction threshold levels of power for the pulse durations of 100 ns, 200 ns and 400 ns are determined to understand the effect of HPM technology in a better way.

In chapter 4, the performances of two diode limiters are evaluated against the HPM threat. Firstly, TGL2201 is exposed to these HPM pulses and the response time of the device is measured as less than 10 ns, which shows that TGL2201 is fast enough to resist to this threat. Nevertheless, maximum power handling capacity is too low for HPM pulses. Secondly, a high power diode, CLA4609, is

investigated in terms of response time. When response time is calculated by using spike leakage value, it is seen that response time is too long. Thus, these evaluations show that the diode technology is not suitable to survive against the HPM technology.

In chapter 5, vanadium dioxide is synthesized with two hydrothermal methods. Then, these synthesized VO_2 samples are characterized by X-ray diffraction technique and the extraction of resistance characteristics of VO_2 samples. These characterization processes prove that the VO_2 samples are produced successfully. The Teledyne's patent [3] describing the VO_2 limiter structure is investigated to realize this device with different dimensions as a prototype. The width of capacitive iris is simulated and varied in HFSS to see the corresponding insertion loss of the limiter. Then, the whole structure is created and simulated in HFSS. In this simulation, the resistance characteristics of samples are also taken into account. After it is observed that this structure can be used as a limiter in the simulation, the first VO_2 limiter is produced in this study. After several trials, it is proved that the device shows a variation in insertion loss during the change of VO_2 state. Some limiters are designed and produced with different thicknesses and different widths of aperture to see the effects of these parameters and to improve the design. Firstly, it is observed that when the thickness of the limiter is decreased from 1 mm to 300 um, the insertion loss of the limiter also diminishes. Next observation is that, the decrease in the width of aperture from 5 mm to 3 mm results in better performance against the same RF pulses. The narrow aperture is heated more effectively with coming HPM pulses, this leads to higher temperature in aperture and so this narrower structure shows better performance. Also, the response time of the limiter is investigated. In these prototypes, the amount of VO_2 material is too large so it is hard to obtain a response time in the order of nanoseconds.

In this thesis, the synthesized VO_2 samples are mostly in metastable structure. However, the monoclinic structure of VO_2 is more successful in the reversible phase transition [19]. Therefore, synthesis of VO_2 in monoclinic form with high

purity could be subject of future work. Another possible future research activity may be to produce thinner prototypes and to use less amount of transition material. This activity could improve insertion loss, isolation and response time of the limiter.

REFERENCES

[1] G. Ni, B. Gao and J. Lu, “Research on high power microwave weapons,” in Proceedings of the Asia-Pacific Microwave Conference, Suzhou, 2005.

[2] T. Nilsson, “Investigation of limiters for HPM and UWB front-door protection”, M.S. thesis, Dept. of Electrical Eng., Linköping University, Linköping, Sweden, 2006.

[3] C. E. Hillman et al.(2011). US. Patent No. 8,067,996 B2. California: U.S. Patent and Trademark Office.

[4] F. Sabath et al. "Overview of four European high-power microwave narrow-band test facilities", IEEE transactions on electromagnetic compatibility, vol.46, no.3, pp. 329-334, 2004.

[5] J. M. Borky, “Vulnerabilities to electromagnetic attack of defense information systems” in: J. S. Gansler and H. Binnendijk, “Information assurance, trends in vulnerabilities, threats and technologies”, National Defense University, Center for Technology and National Security Policy, Washington, 2005, pp.65-92.

[6] F. Morin, “Oxides Which Show a Metal-to-Insulator Transition at the Neel Temperature,” Physical Review Letters. 1959

[7] J. Nag, “The solid-solid phase transition in vanadium dioxide thin films: synthesis, physics and application” Ph.D. dissertation, Faculty of the Graduate School of Vanderbilt Univ., Tennessee, U.S., 2011.

[8] D. Johansson, “VO_2 films as active infrared shutters”, M.S. thesis, Dept. of Applied Physics and Electrical Eng., Linköping University, Linköping, Sweden, 2006.

[9] C. Wu et al. "Direct hydrothermal synthesis of monoclinic VO_2(M) single-domain nanorods on large scale displaying magnetocaloric effect.", Journal of Materials Chemistry 21.12 pp. 4509-4517, 2011.

[10] E. Sovero, D. Deakin, J.A. Higgins, J.F. DeNatale, S. Pittman, "Fast thin film vanadium dioxide microwave switches", 1990 IEEE GaAs IC Symposium Technical Digest, pp. 101- 103, October 7-10, 1990.

[11] D. Bouyge et al., “Applications of vanadium dioxide (VO_2)-loaded electrically small resonators in the design of tunable filters,” Proceedings of the 40th European Microwave Conference, vol. 22, no. 3, pp. 822-825, Sep. 2010.

[12] C. Yang, P. G. Liu, and X. J. Huang, “A novel method of energy selective surface for adaptive HPM/EMP protection” IEEE Antennas and Wireless Propagation Letters, Vol. 12, pp. 112–115, 2013.

[13] P. Kelly, J. Mankowski, M. Kristiansen, “A tunable metamaterial-based passive limiter for protection from HPM and UWB sources”, Pulsed Power, International Conference - PPC , pp. 400-403, 2011.

[14] C. N. Berglund, “Thermal Filaments in Vanadium Dioxide”, IEEE Transactions on Electron Devices, vol. ED-16, No.5, pp.432-437, May 1969.

[15] D. Mansson, R. Thottappillil, M. Backstrom, and O. Lunden, “Vulnerability of European rail traffic management system to radiated intentional EMI”, IEEE Trans. Electromagn. Compat., vol. 50, no. 1, pp. 101–109, Feb. 2008.

[16] T. Nilsson and R. Jonsson, “Investigation of HPM front-door protection devices and component susceptibility,” Swedish Defense Res. Agency (FOI) Tech. Rep., Nov. 2005.

[17] L. Chen et al., “Synthesis of Thermochromic W-Doped VO_2 (M/R) Nanopowders by a Simple Solution-Based Process”, Journal of Nanomaterials Chemistry vol. 2012, June 2012.

[18] C. M. Huang et al., “Sol–gel template synthesis and characterization of VO_2 nanotube,” J. Sol-Gel Sci. Technol., vol. 63, no. 1, pp. 103–107, Apr. 2012.

[19] Kinson C. Kam and Anthony K. Cheetham. "Thermochromic VO_2 nanorods and other vanadium oxides nanostructures." Materials research bulletin 41.5, pp. 1015-1021, 2006

[20] J. Livage, “Hydrothermal synthesis of nanostructured vanadium oxides”, Materials, pp. 4175-4195, July 2010